An Efficient Synthesis, PET Evaluation and Application of [^{18}F]MEFWAY designed for Imaging Brain Serotonin 1A Receptors in Rodents

Jae Yong Choi

Department of Medical Science

The Graduate School, Yonsei University

An Efficient Synthesis, PET Evaluation and Application of [^{18}F]MEFWAY designed for Imaging Brain Serotonin 1A Receptors in Rodents

Directed by Professor Chul Hoon Kim

The Doctoral Dissertation submitted to the

Department of Medical Science

the Graduate School of Yonsei University

in partial fulfillment of the requirements for the degree of Doctor of Philosophy

Jae Yong Choi

December 2012

This certifies that the Doctoral Dissertation of Jae Yong Choi is approved.

Thesis Supervisor: Chul Hoon Kim

Thesis Committee Member #1: Dong Goo Kim

Thesis Committee Member #2: Young Hoon Ryu

Thesis Committee Member #3: Sung-Rae Cho

Thesis Committee Member #4: Gwangil An

The Graduate School

Yonsei University

December 2012

ACKNOWLEDGEMENT

여러 가지로 부족한 제가 학위 논문을 마무리하게 된 것은 오롯이 저를 이끌어주시고 격려해주신 많은 분들의 덕분입니다. 그분들의 도움이 없었더라면 현재의 저도 없었을 것이기에 부족하나마 제한된 이 지면을 통해서 인사를 드리고 싶습니다.

이전까지 화학 실험을 하던 저에게 너무나도 생소한 신경과학이라는 분야에서 연구할 수 있도록 기회를 주시고, 큰 가르침을 주신 유영훈 교수님과 김철훈 교수님께 진심으로 감사 드립니다. 유영훈 교수님께서는 자신의 욕심을 내려놓고 주변 사람들과 원만히 소통할 수 있는 겸양의 지혜를, 김철훈 교수님께서는 가장 가까이에서 지도해주시면서 저의 부족한 부분을 채울 수 있도록 열과 성을 다해 지도해 주셨습니다.

각종 세미나를 통해 자신의 연구를 객관적인 관점에서 조명하고, 타인의 연구에 대해 깊이 성찰할 수 있도록 기회를 주신 약리학교실 김경환 교수님, 안영수 교수님, 김동구 교수님, 이민구 교수님, 박경수 교수님, 김주영 교수님께 감사 드립니다.

논문의 계획단계부터 완성까지 아낌없는 조언을 해주신 조성래 교수님과 '박사'의 의미와 긍정적 사고에 대해 깊은 가르침을 주신 김동구 교수님께 깊은 감사 드립니다.

자주 만나지는 못해도 항상 저를 따뜻하게 맞아준 약리학 교실 손선영, 임영신 박사님, 문여정, 이정호, 권오빈, 한웅수, 조호진, 윤홍인, 신소라, 고석진, 서제호, 윤은장, 오소라 선생님과 이동환, 손한길 선생님께도 고마운 마음을 표현하고 싶습니다.

유기화학과 방사화학을 가르쳐 주신 원자력의학원 이교철 박사님과 안광일 박사님, 소동물 영상을 연구할 수 있는 기회를 제공해주시고 지원해주신 김경민, 최태현 박사님, 약물 동력학과 소동물 전처치를 가르쳐 주신 김병수 선생님, 밤샘까지 마다하지 않고 연구를 도와준 이치훈, 한상진 선생님, 김은정 선생님께 감사 드립니다. 그리고 학부 때부터 지금까지 한결같이 힘이 되어주고 열정적 연구자의 모습을 몸소 보여준 김정영 박사님께 감사 드립니다.

강남세브란스병원 핵의학과 전태주, 이민경 교수님과 김효숙, 김혜원 선생님들에게 감사 드립니다. 한번도 불평하지 않고 항상 웃는 얼굴로 묵묵히 일을 하면서 저를 지원해준 서영범 선생님께 정말 고맙고, 많이 피곤하신데도 불구하고 평일 야간과 주말 임상연구를 지원해주신 PET 방 송태호, 이원택, 전민수, 김택준 선생님과 가속기실 이현일 선생님께도 감사 드립니다.

항상 아들의 위해 기도해 주시는 사랑하는 어머님과 장모님, 멀리 떨어진 동생을 위해 격려를 아끼지 않으신 형님과 형수님, 누나와 매형, 재훈이와 제수씨에게 감사 드립니다. 그리고, 많은 부분을 포기하면서 부족한 남편을 뒷바라지 해주느라 고생한 사랑하는 아내에게도 고마움을 표현하고 싶습니다.

마지막으로 화학에 대한 흥미를 갖게 해주시고, 저를 처음 연구자의 길로 인도해 주신 故 채희권 교수님과 하늘에서 저를 보살펴 주시는 아버지 영전에 이 논문을 바칩니다.

저자 씀.

TABLE OF CONTENTS

ABSTRACT **1**

I. INTRODUCTION **4**

1. The serotonergic system 6

2. The serotonin 1A ($5\text{-}HT_{1A}$) receptor 8

3. Positron emission tomography (PET) 9

4. Radioligands for imaging $5\text{-}HT_{1A}$ recetors 14

5. Neurobiology of depression. 17

6. Serotonergic dysfunction in Parkinson's disease 21

7. Purposes of the research 22

II. MATERIALS AND METHODS **23**

Experiment 1. Synthesis of [^{18}F]MEFWAY **23**

1. Chemicals 23

2. Reaction and purification method 23

3. Spectroscopies 24

4. Radioisotope production 24

5. Radiochemistry 25

6. Quality control 26

Experiment 2. Biological evaluation of [^{18}F]MEFWAY 29

1. Materials and methods 29

2. Animals 30

3. PET experiment 30

4. Image analysis 31

Experiment 3. Application to animal disease models 33

1. Acute model for depression 33

2. Parkinson's disease model 35

III. RESULTS 38

Experiment 1. Synthesis of [^{18}F]MEFWAY 38

1. An efficient synthesis of [^{18}F]MEFWAY precursor 38

2. Synthesis of non-radioactive MEFWAY and WAY-100635 45

3. Radiosynthesis of [^{18}F]MEFWAY 47

4. Quality control of [^{18}F]MEFWAY 50

Experiment 2. Biological evaluation of [^{18}F]MEFWAY 51

1. Metabolic stability of [^{18}F]MEFWAY 51

2. Specificity of [^{18}F]MEFWAY to 5-HT$_{1A}$ receptors 57

Experiment 3. Application to animal disease models 59

1. Acute model for depression 59

2. Parkinson's disease model 64

IV. DISCUSSION **68**

1. Synthesis of [^{18}F]MEFWAY precursor 68

2. The advantages of [^{18}F]MEFWAY 70

3. Biological evaluation of [^{18}F]MEFWAY 72

3. Application to animal disease model 74

V. CONCLUSION **77**

REFERENCES **79**

ABSTRACT (IN KOREAN) **95**

LIST OF FIGURES

Figure 1. Biosynthesis and degradation of serotonin 7

Figure 2. ^{18}F-based radiotacers synthesized using electrophilic substitution..... 12

Figure 3. ^{18}F-based radiotacers synthesized using nucleophilic substitution. 13

Figure 4. Representative PET radioligands for imaging 5-HT_{1A} receptors. 16

Figure 5. Synthetic scheme of [^{18}F]MEFWAY precursor..... 39

Figure 6. Confirmation and analysis of [^{18}F]MEFWAY following radiosynthesis. 49

Figure 7. Time-activity curves of [^{18}F]MEFWAY uptake in skull for control and various dosages of inhibitors, fluconazole and miconazole. 52

Figure 8. PET images of [^{18}F]MEFWAY uptake in skull and brain for control and various dosages of inhibitors, fluconazole and miconazole. 53

Figure 9. Time-activity curves of [^{18}F]MEFWAY in specific brain regions for various dosages of fluconazole 55

Figure 10. Ratio of [^{18}F]MEFWAY specific to non-specific binding curves in the hippocampus 56

Figure 11. Pre-block and displacement experiments with non-radioactive WAY-100635..... 58

Figure 12. Representative PET images of [^{18}F]MEFWAY in the control and the forced swimming stressed rat..... 60

Figure 13. Time-activity curves of [^{18}F]MEFWAY uptake in specific regions of the brain for the control and the forced swimming stress group (despair group) .. 61

Figure 14. Comparison of the BP_{ND} of [^{18}F]MEFWAY in the hippocampus between the control and the forced swimming stress group (despair group) 62

Figure 15. Correlation between [^{18}F]MEFWAY BP_{ND} in the hippocampus and immobility in the forced swimming stress group (despair group). 63

Figure 16. Representative PET images of [^{18}F]MEFWAY in the control and the 6-OHDA lesioned rat 65

Figure 17. Time-activity curves of [^{18}F]MEFWAY uptake in the specific regions of the brain for the control and the 6-OHDA lesion group 65

Figure 18. Comparison of [^{18}F]MEFWAY BP_{ND} in the hippocampus between the 6-OHDA lesion and the control group 66

Figure 19. Comparison of reaction mechanisms between BOP and oxalyl choride based reaction..... 68

LIST OF TABLES

Table 1. Comparison of nucleophilic and electrophilic substitution reactions..... 13

Table 2. Current research statuses of PET radioligands for imaging 5-HT_{1A} receptors..... 16

Table 3. Quality control parameters in [^{18}F]MEFWAY..... 50

ABSTRACT

An Efficient Synthesis, PET Evaluation and Application of [^{18}F]MEFWAY designed for Imaging Brain Serotonin 1A Receptors in Rodents

Jae Yong Choi

Department of Medical Science

The Graduate School, Yonsei University

(Directed by Professor Chul Hoon Kim)

The changes of serotonin 1A (5-HT_{1A}) receptor density in the central nervous system are related to various psychiatric disorders such as depression, anxiety and schizophrenia. Thereby *in vivo* imaging of brain 5-HT_{1A} receptors has been an important subject in neuroscience.

Recently, 4-([^{18}F]fluoranylmethyl)-*N*-[2-[4-(2-methoxyphenyl)piperazin-1-yl]ethyl]-*N*-pyridin-2-ylcyclohexane-1-carboxamide ([^{18}F]MEFWAY) was developed as a positron emission tomography (PET) radioligand for quantifying the 5-HT_{1A} receptors. *Ex vivo* autoradiography of [^{18}F]MEFWAY represented a high affinity and selectivity to the 5-HT_{1A} receptors. However, there is no report on testing its biochemical and pharmacological characteristics *in vivo* due to the low synthetic yield of its precursor. Here, I increased the synthetic yield of the [^{18}F]MEFWAY precursor and studied the effectiveness of [^{18}F]MEFWAY *in vivo*.

First of all, I established an efficient synthetic method for the [^{18}F]MEFWAY precursor, which consists of the improved acid chloride coupling reaction to activate the carboxylic acid and optimized reduction condition to suppress the breakdown of the amide bond. This new protocol dramatically improves the synthetic yield compared to the previous method (<8% → 45%).

After F-18 was incorporated into the precursor, metabolic stability against defluorination and efficacy of [^{18}F]MEFWAY were assessed in the rat brain. Unexpectedly, [^{18}F]MEFWAY showed severe skull uptake due to the defluorination. It is known that cytochrome P450 2E1 is a major metabolizing enzyme that causes *in vivo* defluorination of ^{18}F-based radioligands and can be suppressed by antifungal drugs (i.e. miconazole and fluconazole). The skull uptake of [^{18}F]MEFWAY was suppressed by the pretreatment of miconazole and fluconazole up to 68% or 80%, respectively. Then, I confirmed the specificity of [^{18}F]MEFWAY to 5-HT_{1A}

receptors by the pre-block and displacement experiments using a highly selective 5-HT_{1A} antagonist.

Finally, I tested the utility of [^{18}F]MEFWAY in animal disease models. Unilateral 6-OHDA lesion and forced swimming were respectively used to evoke Parkinson's disease model and the acute model for depression. In the unilateral 6-OHDA lesion rats, binding potential in the hippocampus was significantly reduced bilaterally compared with that of the control. The acute model for depression also exhibited significant decrement of binding potential in the hippocampus.

These results suggested that [^{18}F]MEFWAY is a useful PET radioligand to examine the changes of 5-HT_{1A} receptor density *in vivo*.

Keywords: 5-HT_{1A} receptor, PET, radioligands, depression, Parkinson's disease

Efficient Synthesis, PET Evaluation and Application of [^{18}F]MEFWAY designed for Imaging Brain Serotonin 1A Receptors in Rodents

Jae Yong Choi

Department of Medical Science

The Graduate School, Yonsei University

(Directed by Professor Chul Hoon Kim)

1. INTRODUCTION

Serotonin 1A (5-HT_{1A}) receptors in the central nervous system (CNS) are located in both the midbrain and the limbic system. The alteration of these receptor densities has been strongly associated with various neuropsychiatric disorders such

as anxiety[1-3], depression[4,5] and schizophrenia[6]. Therefore, the importance of a molecular imaging agent for 5-HT_{1A} receptors in living systems has been increasingly recognized[7,8].

Positron emission tomography (PET) can quantify the distribution of protein molecules such as receptors and transporters in the brain *in vivo*. It directly correlates to other *in vitro* techniques such as receptor autoradiography, Western blots, and Northern blots[9].

Although many PET radioligands have been developed for imaging 5-HT_{1A} receptors, there are no routinely applicable radioligands in pre-clinical or clinical studies. Recently, [^{18}F]MEFWAY has been developed as a promising radiocompound, in which high specific binding to the receptors and excellent signal to noise ratio has been observed. However, so far, reliable reports about its efficacy *in vivo* have not been published due to the improper synthetic method of its precursor.

The overall aims of this study are to establish an efficient synthetic method for the MEFWAY precursor, then to assess the efficacy of [^{18}F]MEFWAY in small animals.

1. The serotonergic system

A. Serotonin

Serotonin (5-hydroxytryptamine, 5-HT) was first isolated as an unknown vasoconstrictor in serum, secreting from platelets during blood clotting. In 1984, Rapport identified that this substance is the serotonin from the bovine serum[10]. At about the same time, Erspamer had discovered the smooth muscle contracting substance from the gut mucosa, then named it enteramine because the enterochromaffin cells of the gastrointestinal tract have larger amounts of this substance[11]. In 1953, Erspamer and Asero had demonstrated that serotonin and enteramine are identical[12]. Afterward, Twarog and Page detected serotonin from brain extracts[13]. Since then, serotonin has been recognized as a contracting factor and neurotransmitter.

5-HT is found in the gastrointestinal tract, blood and CNS. Firstly, about 90% of all serotonin is present in the enterochromaffin cells that are dispersed in mucosal cells. In this area, 5-HT promotes gastrointestinal motility and contraction of isolated strips of intestine. Secondly, about 8% of 5-HT is present in platelets and helps platelet aggregation. The remaining 5-HT (2%) is located in the CNS and it regulates various brain functions such as mood, appetite, sleep and cognitive functions.

In the brain, serotonergic neurons synthesize its own 5-HT because it does not cross the blood-brain barrier. Firstly, L-tryptophan, which is delivered from diet, is hydroxylated by the tryptophan hydroxylase (TPH) generating 5-hydroxy-L-tryptophane (5-HTP). Then, decarboxylation of the 5-HTP by aromatic L-amino acid decarboxylase (AADC) gives the 5-HT. This 5-HT is transported from the cytoplasm and it is stored in synaptic vesicles by the vesicular monoamine transporter 2 (VMAT2). After the release of 5-HT into the synaptic cleft, it will interact with the 5-HT receptors. Then, 5-HT undergoes reuptake in the presynaptic neuron through serotonin reuptake transporters. The 5-HT in the brain is metabolized to 5-hydroxyindoleacetic acid (5-HIAA) by the monoamine oxidase (MAO) and aldehyde dehyrogenase in the nerve ending. Finally, 5-HIAA is excreted in the urine and serves as an indicator of 5-HT production in the body[14]. Biosynthesis and degradation of 5-HT is illustrated in Figure 1.

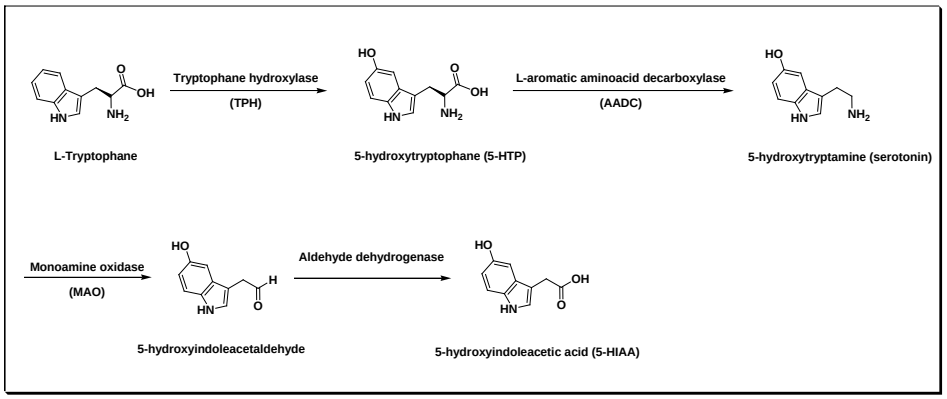

Figure 1. Biosynthesis and degradation of serotonin.

B. Serotonergic pathways in the brain

The cell bodies of 5-HT neurons are located in the raphe nuclei and the serotonergic systems are divided into two tracts. In the caudal serotonergic system, 5-HT neurons in the raphe nuclei project to the spinal cord. For the rostral serotonergic system, the cell bodies in the raphe nuclei innervates to several regions in the forebrain, including the basal ganglia and limbic system[15].

2. The serotonin 1A (5-HT_{1A}) receptor

To date, 7 structurally and pharmacologically different receptor subtypes (5-HT_{1-7}) have been identified and these subfamilies have been re-assigned into 14 subtypes[16]. All 5-HT receptor subtypes are G-protein coupled receptors except the 5-HT_3 that is a ligand gated sodium ion channel. The transmembrane stretches are linked by three extracellular loops and three intracellular loops. The amino acid sequences of all 5-HT receptors have a high degree of homology at the transmembrane domains. In contrast, the sequences of the N-terminal portion and the third intracellular loop are rather unique for each given receptor.

Among these, the 5-HT_{1A} receptors are the most widely investigated receptor because they modulate global 5-HT system activity and the involvement of 5-HT_{1A}

receptors has been demonstrated in several psychiatric disorders. These receptors are universally distributed throughout the CNS. They are localized in the cerebral cortex, hippocampus, septum, and raphe nucleus in high densities, while in very low amounts in the striatum, substantia nigra and the cerebellum. The 5-HT_{1A} receptors in the raphe nuclei exist in the cell bodies and dendrites of 5-HT neuron and hence are called somatodendritic autoreceptors. In the presynaptic site, they work as reuptake modulators of the synaptic 5-HT causing a decrease in the release of 5-HT into terminal fields. 5-HT_{1A} receptors are also located postsynaptically in the cortical and limbic area[17-19].

3. Positron emission tomography (PET)

A. Characteristics of PET

PET, a non-invasive imaging technique, provides biological and physiological information from living systems. A major advantage of PET is its high sensitivity (10^{-9}-10^{-12} M) that allows for detection of the interactions between radioligands and their protein targets. This sensitivity is many orders of magnitude greater than the sensitivity with magnetic resonance imaging (MRI) (~10^{-4} M), or computed tomography (CT)(~10^{-3} M)[8,20].

The PET system detects pairs of gamma rays emitted indirectly by positron emitting radionuclides. In general, PET uses radiocompounds in which one or more atoms of bioactive molecules have been replaced by radioisotopes. The representative PET isotopes are ^{11}C, ^{13}N, ^{15}O, ^{18}F and a particle accelerator called cyclotron produces these radioisotopes.

Of these, I focused on F-18 based radiocompounds because of their exclusive advantages over the others. Firstly, F-18 has a relatively long half-life (110min) allowing enough time to synthesize the radiocompounds. This characteristic also permits transport of the radiocompounds to considerable distances, from the laboratory to the patients. Secondly, F-18 can substitute the hydrogen or hydroxyl groups of the biologically active molecules without appreciably affecting biological functions in the living system. Moreover, fluorine has a bond strengthening effect on the neighboring carbon frame, allowing fluorinated compounds to show higher metabolic, oxidative and thermal stability[21].

B. Fluorine-18 Radiochemistry

High specific activity (i.e. ratio of [^{18}F]fluoride ion radioactivity to its mass of other substance called carrier) is mandatory for radioprobes that are targeted at

protein targets in the brain, because low specific radioactivity (high carrier) would saturate the target proteins with non-radioactive ligands and so would nullify the signals from the radiotracers. High specific radioactivity enables radiotracers to be administered to living subjects in low mass doses (typically less than 1-10 nmol) without any toxic or pharmacological effects.

Syntheses using ^{18}F need to be quick and efficient due to its limited half-life. There are two methods for the preparation of ^{18}F-based radiocompounds[22 23].

(1) Electrophilic substitution

^{18}F-labeling reactions utilizing electrophilic substitution use $[^{18}F]F_2$ produced by a cyclotron. Proton irradiation of ^{18}O leaves ^{18}F attached to the target walls, which is extracted by F_2 gas (carrier), resulting in ^{18}F-F. The theoretical maximum radiochemical yield is limited to 50% because we only use the radioactive ^{18}F from the ^{18}F-F.

Electrophilic methods have low synthetic yield given undesired radical side reactions with solvents. Hence, this method is requires extensive purification procedures. Recently attempts were made to reduce the amount of fluorine carrier in the synthesis of electrophilic ^{18}F-based radiocompounds. Higher specific activities

were obtained via electric gaseous discharge of [^{18}F]methylfluoride than the previous method. This, however, also has low radiochemical yields.

Although electrophilic substitution has these drawbacks, the synthesis of [^{18}F]fluoro-L-DOPA and 2-L-[^{18}F]fluorotyrosine still rely on this protocol.

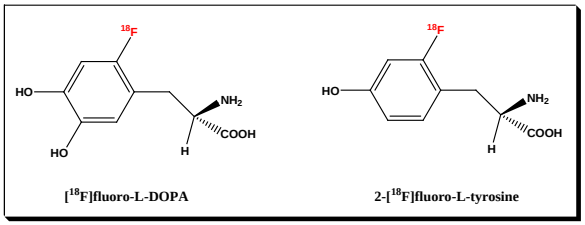

Figure 2. ^{18}F-based radiotacers synthesized using electrophilic substitution .

(2) Nucleophilic substitution

^{18}F-labeling reactions utilizing nucleophilic substitution use ^{18}F ion produced via the ^{18}O(p,n)^{18}F nuclear reaction in a cyclotron, without requiring a carrier addition. This process results in the formation of [^{18}F]HF due to the high charge density of ^{18}F ion. [^{18}F]HF makes ^{18}F unavailable for further reactions. To overcome this drawback, [^{18}F]HF can be passed through an anion exchange resin, which traps the ^{18}F ion. The ^{18}F ion is then extracted from the anion exchange resin with an aqueous basic solution.

The main attraction of this method is that the fluorine-18 is obtained in a no-carrier-added (NCA) form. This means the [^{18}F]fluoride ion has a very high specific radioactivity and has a higher radiochemical yield than the electrophilic substitutions due to the simplified synthetic purification steps. Therefore, nucleophilic ^{18}F-fluorination is currently the most common synthetic method. For example, such radioprobes are synthesized through nucleophilic flourination: [^{18}F]FDG[24] for glucose metabolism, 3'-deoxy-3'-[^{18}F]fluorothymidine ([^{18}F]FLT)[25] for DNA proliferation, [^{18}F]fallypride[26] for dopamine D2 receptors, and [^{18}F]fluoromisonidazole ([^{18}F]FMISO) for hypoxia study[27].

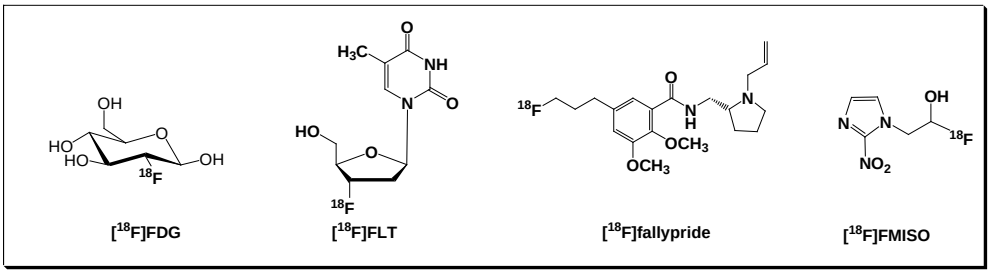

Figure 3. ^{18}F-based radiotacers synthesized using nucleophilic substitution.

Table 1. Comparison of nucleophilic and electrophilic substitution reactions.

	Nucleophilic reaction	Electrophilic reaction
Target	$H_2{}^{18}O$	$^{18}O_2$, Kr (50 μmol F_2)
Main product	$^{18}F^-$ (aqueous)	[^{18}F]F_2
Specific activity (MBq/μmol)	600 x 10^3	600

4. Radioligands for imaging 5-HT_{1A} receptors

In order to generate quantifiable images of brain 5-HT_{1A} receptors, radioligands must fulfill certain properties[28]. Primarily, radiosynthesis should be simple and reproducible. Secondly, the radioligands must possess high selectivity and affinity toward the target of interest to maximize the signal to noise ratio. Thirdly, radioligands have to be moderately lipophilic to ensure adequate penetration of the blood brain barrier (BBB). Lastly, the radioligands should not generate troublesome metabolites that interfere with the quantification of radioactivity from parent radioligands in the target region because PET has no way to discriminate between the radioactivity of parent radioligands and that of radiometabolites.

Many radioligands have been developed for imaging 5-HT_{1A} receptors and most of these tracers belong to the structural families of [*N*-(2-(1-(4-(2-methoxyphenyl)-piperazinyl)ethyl))-*N*-(2-(pyridinyl))cyclohexanecarboxamide] (WAY-100635), which is a selective and high-affinity 5-HT_{1A} receptor antagonist (K_D = 0.2 - 0.4 nM)[29-36]. Among these, only three radioligands have been applied in human studies: [*carbonyl*-^{11}C]WAY-100635, [^{18}F]*trans*-4-fluoro-N-2-[4-(2-methoxyphenyl)piperazin-1-yl]ethyl]-*N*-(2-pyridyl)cyclohexanecarboxamide ([^{18}F]FCWAY), and 4-[^{18}F]fluoranyl-*N*-[2-[4-(2-methoxyphenyl)piperazin-1-yl]ethyl]-N-pyridin-2-ylbenzamide ([^{18}F]MPPF) (Figure 2, Table 1). Nevertheless [*carbonyl*-^{11}C]WAY-100635 is by far the most utilized PET radioligand. This radiocompound, however, shows fast

systemic metabolism, which makes assessing available receptor density difficult[37]. Afterward, [^{18}F]FCWAY had been developed, yet only one research institute used this radioprobe in rat and human subjects[38-40]. This radioligand undergoes significant defluorination *in vivo* through the activation of cytochrome P450 2E1 (CYP2E1) isozyme in the liver[40,41]. This defluorination hampers the exact quantification of receptor density due to a spillover effect, in which radioactivity in the skull can be also detected in brain regions nearby, such as the cortex.

[^{18}F]MPPF was developed as a high selective 5-HT$_{1A}$ antagonist without defluorination *in vivo*. The drawback of [^{18}F]MPPF is that it is an avid substrate for P-glycoprotein (P-gp). P-gp in the BBB acts as an efflux pump and repels many xenobiotic compounds. Thus, most radioactivities from [^{18}F]MPPF are excluded from the brain and only 10% of injected [^{18}F]MPPF is detected in the brain compared with [*carbonyl*-^{11}C]WAY-100635 in rat. Recently, Saigal et al. developed a very promising radioligand for human subjects, [^{18}F]MEFWAY, which has similar binding affinity and selectivity to 5-HT$_{1A}$ receptors as [*carbonyl*-^{11}C]WAY-100635[42]. However, the [^{18}F]MEFWAY research had not yet expanded beyond a single institute possibly due to the low synthetic yield of its precursor. Until now, no research regarding the *in vivo* biological characteristics of [^{18}F]MEFWAY has been conducted[43].

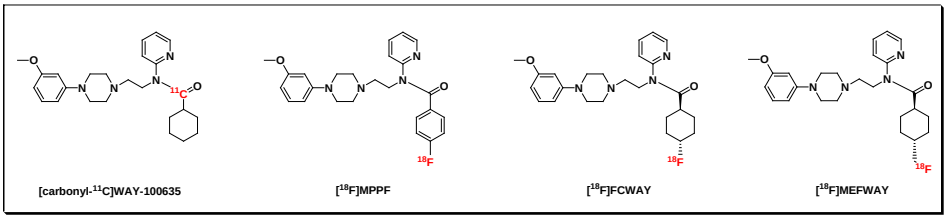

Figure 4. Representative PET radioligands for imaging 5-HT_{1A} receptors.

Table 2. Current research statuses of PET radioligands for imaging 5-HT_{1A} receptors.

Radioligands	R	H	Ongoing	Problem	Research institutions
[*carbonyl*-^{11}C] WAY-100635	√	√	√	Fast metabolism	12
[^{18}F]MPPF	√	√	√	Low brain uptake	6
[^{18}F]FCWAY	√	√	√	Defluorination, Low yield	1
[^{18}F]MEFWAY	ND	ND	ND	Low yield	1

(R: rodent, H: human)

√ indicates that *in vivo* PET studies were performed. "Ongoing" indicates that the ligand is still being used for research. ND indicates not yet determined.

5. Neurobiology of depression

Depression is a common mental disorder that characterized by inability to feel pleasure (anhedonia), low self-esteem, impairment of sleep or appetite, and poor concentration. It is a heterogeneous syndrome composed of numerous diseases of distinct causes and pathophysiologies. Several hypotheses on the symptoms of depression have been suggested based on dysregulation of the hypothalamic pituitary-adrenal axis, brain derived neurotrophic factor, cyclic-AMP response element binding protein and serotonergic system.

A. Hyperactivation of the hypothalamic pituitary-adrenal (HPA) axis[44]

When an organism is exposed to a stressor, the hypothalamic-pituitary-adrenal (HPA) axis is activated. Neurons in the paraventricular nucleus (PVN) of the hypothalamus release a corticotrophin-releasing factor (CRF). The CRF stimulates the synthesis and secretion of adrenocorticotrophin hormone (ACTH) from the anterior pituitary. ACTH then stimulates the glucocorticoid-producing adrenal cortex.

The activity of the HPA axis is controlled by the hippocampus that exerts an inhibitory influence on hypothalamic CRF-containing neurons and by the amygdala, which exerts an excitatory influence.

Glucorticoids, by potently regulating hippocampus and PVN neurons, exert powerful feedback effects on the HPA axis. In normal physiological conditions, hippocampal inhibition of HPA activity is enhanced. However, in severely stressful circumstances, the inhibitory ability of the hippocampus on the HPA axis is reduced generating increased glucocoticoid levels and subsequent hippocampal damage.

Glucocorticoids inhibit cytokine production. For example, glucocorticoids directly decrease transcription of the genes for interleukin-6 (IL-6) and interleukin-1β, thus decreasing their production by immune cells. In addition, immune response is indirectly suppressed by glucocorticoids through inhibition of pro-inflammatory transcription factors such as nuclear factor-κβ (NF- κβ) and activating protein-1 (AP-1).

The hyperactivation of the HPA axis is observed in approximately half of individuals with depression, and these abnormalities are corrected by antidepressant treatment.

B. The Brain-derived neurotrophic factor (BDNF)

BDNF is one of the most prevalent neurotrophic factors in adult brains and it has the ability to support the survival of a subset of peripheral neurons during development[45]. Recently, the changes in BDNF level have been implicated in the etiology of depression. Several clinical studies have reported that serum BDNF levels are reduced in depressed patients[46,47].

In the pituitary gland and the hippocampus, BDNF expression is regulated by stress and glucocorticoid. For example, acute and chronic stress decrease levels of BDNF expression in the dentate gyrus and pyramidal cell layer of hippocampus in rodents[48].

Although the findings about the association of serum BDNF levels and depression are remarkably robust, it is unclear whether serum BDNF levels might reflect or contribute to the BDNF levels in brain.

C. Cyclic-AMP response element binding protein (CREB)

CREB is a member of the basic leucine zipper family of transcription factors. It plays an important role in the development of the nervous system and depression[49].

Ren et al. reported that a significant correlation exists between CREB protein levels and the Hamilton depression rating scale (HDRS) that provides an indication of the level of a patient's depression[50]. In addition, the protein and mRNA expression of CREB significantly decreased in the prefrontal cortex and hippocampus of depressed suicide victims compared with controls.

D. Serotonergic system

There is extensive studies suggest that the dysfunction of the serotonergic system play a causal role in the depression. The most reliable evidences are the effect on lowering brain 5-HT concentration in the patients with depression due to the increased MAO-A activity[51], which is responsible of the metabolism of the 5-HT. The levels of tryptophan in plasma and 5-HIAA in the cerebrospinal fluid (CSF) were also decreased in depressive patients[52,53].

Alteration of the 5-HT_{1A} receptor density is an important role in the pathophysiology of the depression because 5-HT_{1A} receptors are abundance in the limbic system and they maintain 5-HT concentration in the brain. Postmortem studies in the depressive patients reported that 5-HT_{1A} receptor mRNA levels were reduced in the hippocampus and receptor density was reduced in the prefrontal cortex[54,55]. PET studies using [^{11}C]WAY-100635 reported that the down regulation

of 5-HT_{1A} receptors was observed in the raphe nuclei, anterior cingulate and mesiotemporal cortices[4,5].

6. Serotonergic dysfunction in Parkinson's disease

Parkinson's disease (PD) is a common neurodegenerative disorder and is clinically characterized by the motor symptoms of tremor, bradykinesia, and rigidity as well as by the non-motor symptoms of physiological processes, which are mainly mediated in the serotonergic system.

Postmortem, pathological and functional imaging studies have demonstrated serotonergic dysfunction in PD. In postmortem studies of patients with PD, serotonin depletion was observed at the caudate as well as frontal cortex[56,57]. A pathological study showed preferential loss of 5-HT in the caudate compared with the putamen, but with relatively low loss of 5-HT (66%) than dopamine (99%)[58]. Imaging studies *in vivo* have also suggested the depletion of 5-HT innervations to the striatum measured via decreased serotonin transporter binding[59,60]. In addition, midbrain raphe 5-HT_{1A} binding in the depressed patients was reduced by 27% with [^{11}C]WAY-100635 PET[61].

7. Purposes of the research

The purposes of this study were to establish an efficient synthetic method of [^{18}F]MEFWAY precursor, to assess the efficacy of [^{18}F]MEFWAY *in vivo* and to test the utility of the radioprobe in the acute model for depression and Parkinson's disease model.

II. MATERIALS AND METHODS

Experiment 1. Synthesis of [^{18}F]MEFWAY

1. Chemicals

Trans-4-carbomethoxycyclohexane-1-carboxylic acid was obtained from Rieke Metals, Inc, USA. Silica Gel 60N for the gravity column chromatography was purchased from the Kanto Chemical Co., Inc., Tokyo. [^{18}O]water was purchased from Rotem, Israel. Other solvents and starting materials for synthesis were purchased from Sigma-Aldrich (St. Louis, MO, USA) and used as received without purification.

2. Reaction and purification method

Reactions were performed under Argon atmosphere and anhydrous solvents were used. Thin layer chromatography (TLC) was run on the pre-coated glass plates of

silica gel 60F 254 (Merck, Germany). After reaction, the compounds were exposed to UV-lamp (254nm, Spectroline, USA) and by dipping the TLC-plates in a 1% aqueous $KMnO_4$ solution. Flash column chromatography was conducted on silica gel 0.040- 0.063 mm (Merck, Germany).

3. Spectroscopies

NMR spectra were obtained on a Bruker Advance 500 MHz instrument (Germany) using a deuteriated solvent and chemical shifts are reported in ppm relative to the deuterated solvent ($CDCl_3$, δ = 7.25 ppm for ^{1}H NMR and δ = 77.0 ppm for ^{13}C NMR). Spin-spin splitting was represented by singlet (s), doublet (d), triplet (t), and multiplet (m), respectively and coupling constant *J* was calculated by the distance between split peaks multiplied by the field strength in MHz (i.e. 500 MHz for ^{1}H and 125 MHz for ^{13}C). Mass spectra were recorded on a JMS-AX505WA (JEOL, Japan) in the positive-ion mode, using *m*-nitrobenzyl alcohol (*m*NBA) as a fast atom bombardment (FAB) matrix.

4. Radioisotope production

No-carrier-added aqueous [^{18}F]fluoride ion was produced by Eclipse-HP cyclotron (Siemens, Germany) by irradiation of a 2.4 mL water target using a 11

MeV proton beam on 95% enriched [^{18}O]water. Typical production: 1300 mCi (48.1 GBq) of [^{18}F]F^- at the end of bombardment for a 55 μA, 30 min irradiation.

5. Radiochemistry

Radiochemical yields and the identification of the radiocompound were determined with radio-thin layer chromatography (radio-TLC, AR-2000,. Bioscan, Washington D.C. USA). The measurement of radioactivity was determined with CRC 25PET dose calibrator (Capintec, USA). Solid phase extraction was performed using Sep-Pak Cartridges (Waters, USA) such as quaternary methylamine (QMA) and C-18. Kryptofix 222 (K222) was obtained from ABX advanced biochemical compounds (Germany).

High performance liquid chromatography (HPLC) was performed using a YL-9100 system consisting of YL9101 vacuum degasser; YL9110 quaternary pump; YL9120 UV/Vis detector; YL9160 PDA detector (Young Lin, Korea) with Flow-Count radio HPLC detector system (Bioscan FC3300, Washington DC, USA) and manual syringe injector (Rheodyne 7725i with 1.0 mL loop, Rohnert, CA, USA) .

For the purification of the radiochemical synthesis, a preparative reverse phase C-18 column (10μm, 10 x 250m, Waters, Ireland) was used. The preparative column

was eluted at a flow rate of 5 mL/min with a mixture of acetonitrile and water containing 1% v/v triethylamine (TEA) (45:55).

Sterile-filtration of the [^{18}F]MEFWAY was performed by a 0.22 μm membrane filter (Millipore, Millex GS filter unit, Ireland). The specific activity was obtained by integrating the UV absorbance peak corresponding to the radiolabelled product after re-injection of the collected product and followed by the conversion to GBq/μmol from the standard calibration curve.

6. Quality control

A. Visual inspection

The product vial was examined behind a PET L-type lead block. [^{18}F]MEFWAY was required to be clear, colorless, and free of particles.

B. pH

The pH was determined by applying small volume (0.1 mL) of the [^{18}F]MEFWAY to a pH-indicator strip (pH range: 0.0-14.0) and compared by visual

inspection to the color scale provided the test manufacturer. Acceptance criteria were between pH 4.5 and 7.5.

C. Radiochemical purity and radiochemical identity

Radiochemical purity and identity were determined using a radio-TLC scanner and radiochemical identity was confirmed by Younglin HPLC equipped with a UV detector (254nm) and a Bioscan FC3300 radioactivity detector. Non-radioactive MEFWAY was used as a reference standard. Radiochemical identity was confirmed and quantified by calculating the relative retention time (relative retention time, RRT = (retention time of [^{18}F]MEFWAY)/(retention time of MEFWAY), and was required to be 0.9 - 1.10.

D. Radionuclidic purity

Radionuclide purity was analyzed by multi channel analyzer (Seiko EC&G MCA, Tokyo, Japan) to test for the presence of long-lived radioactive contaminants. Acceptance criterion was 511 or 1022 KeV.

E. Residual solvent analysis

The quantity of residual solvent (i.e. acetonitirile) was analyzed by a Younglin GC 6000 with a flame ionization detector (FID) and a DB-WAX column (length 30 m, Inside diameter 0.32 mm, film thickness 0.25 μm). Acceptance criterion was below 400 ppm for acetonitrile.

F. Bacterial endotoxins

Endotoxin content was determined using a Charles River Laboratories EndoSafe Portable Testing System. Maximum recommended dose was required to contain < 175 endotoxin units (EU).

Experiment 2. Biological evaluation of [^{18}F]MEFWAY

1. Materials and Methods

Hepatic CYP450 (CYP) constitutes a super family of heme-containing enzymes that plays an important role in the metabolism of endogenous compounds, such as steroid hormones, biliary salts and fatty acids, as well as the detoxification of xenobiotics[64]. Imidazole and its derivatives are also known to be powerful ligands of the heme iron component of CYP450[65]. In addition, these inhibitors generated reactive intermediates that were irreversibly or quasi-irreversibly bound to the enzyme.

Miconazole and fluconazole were used as antifungal drugs[66-68]. In detail, isotonic aqueous fluconazole was obtained from JW pharmaceutical (2 mg/mL in saline, One Flu injection, JW pharmaceutical, Korea), and miconazole nitrate (2 mg) was dissolved in ethanol (50 μL), polyethyleneglycol (PEG) 400 (650 μL) and saline (300 μL) in sequence for intravenous infusion (2mg/mL).

2. Animals

All animal studies were approved by the committee for the care and use of laboratory animals of Yonsei University College of Medicine. Male Sprague-Dawley rats (280 - 320 g) supplied by Orient Bio, Inc. (Korea) were used for the microPET study. The rats were housed in a temperature and humidity-controlled room with a 12 h light/dark cycle, and free access to food and water.

3. PET experiment

PET scanning was performed with a Siemens Inveon small animal PET scanner (Siemens Medical Solutions). The scanner has a peak absolute system sensitivity of ≥10% in the 250-750 keV energy window, an axial field of view of 12 cm, 1.4 mm full width at half maximum (FWHM) spatial resolution at center of field of view and a transaxial field of view of 10 cm. Anesthesia was induced with 2.5% isoflurane and was maintained during the PET experiment with 1.5% isoflurane for 3 hours. After cannulation in a tail vein, rats were positioned in the center of a gantry. Tracer accumulation in the brain was investigated by dynamic PET scans over 120 min after injection of 15 to 20 MBq of [^{18}F]MEFWAY. Paired rats were

used as controls in this and all other experiments. Attenuation corrections were performed using data from a 10 min transmission scan with a ^{57}Co point source before tracer injection.

4. Image analysis

PET data were reconstructed in user-defined time frames (10 sec x 6 frames, 30 sec x 8 frames, 300 sec x 5 frames, 1800 sec x 3 frames) with a voxel size of 0.861386 x 0.861386 x 0.796000 mm by a 2-dimensionalorder-subset expectation maximization (OSEM) algorithm (4 iterations and 16 subsets). Image files were evaluated by region-of-interest (ROI) analysis using the AsiProVM (Acquisition Sinogram Image Processing software, CTI Concorde Microsystems). ROIs associated with the frontal cortex (FC), hippocampus (HP) and cerebellum (CB) were drawn on all brain coronal images, guided by stereotactic coordinates[69]. The decay-corrected time activity curves are presented in units of the standardized uptake value (SUV) and calculated as (% injected dose/cm^3) x body weight (g) to normalize for the differences in rat weight and administered dose.

Non-displaceable binding potential (BP_{ND}), which is commonly used as an indicator of receptor binding density, is the ratio of the peak values of specific

binding curve (SUV_{ROIs} - SUV_{CB}) divided by the non-specific binding curve (SUV_{CB}) at the time of the peak based on the transient equilibrium method. When the computed specific binding was negative, a value of zero was assigned.

The cerebellum was used as the reference region because it contains very few 5-HT_{1A} receptors in adult rats[70,71]. The demarcation line between the foramen magnum, which is a large hole in the base of the skull, and the cerebellum is indefinite in the PET image. Therefore, I carefully defined the cerebellum as the region apart from the foramen magnum with the lowest radioactivity uptake in the PET image. This cerebellum was used as the ROI to preclude the effect of the skull uptake.

Experiment 3. Applied to the animal disease models

1. Acute model for depression

A. Animals

Fifteen female Sprague-Dawley rats were used. All animal studies were approved by the committee for the care and use of laboratory animals at Yonsei University College of Medicine. The rats were housed in a temperature and humidity controlled room with a 12 h light/dark cycle, and with free access to food and water.

The animals were divided into two groups (control and despair group) and used for *in vivo* imaging of microPET. Seven female Sprague-Dawley rats (420.85 ± 10.30 g, mean ± SD) were subjected to the forced swimming and eight female Sprague-Dawley rats (383.38 ± 10.23 g, mean ± SD) were used as controls.

B. Induce the acute model for depression

Each rat was placed in vertical tank (90 cm height x 20 cm in diameter) containing water (26^{o}C to a depth of 37 cm). The protocol consisted of two

procedures: first, forced swimming for 15 min and 24h later, a second forced swim for 5min. During the second session, the motions of the rats were recorded by a video camera. These recordings were subsequently analyzed for the immobility. The duration of immobility was evaluated by commercial software (Smart, Panlab Harvard apparatus, Spain).

The total duration of immobility behavior was measured during the test session. The water was replaced between the tested individual rats to avoid methodological artifacts like the existence of pheromones or other products excreted by the rats. After each session, the rat was dried with a towel and anesthetized with 2% isoflurane.

C. PET experiment & image analysis

Same procedure as Experiment II (Biological evaluation of [^{18}F]MEFWAY, p. 20).

D. Statistical analysis

All data were presented as mean ± standard error of the mean (SEM). The differences in BP_{ND} were analyzed with Student's unpaired t-test. The correlation

coefficient between the control and the despair group was analyzed with Pearson's correlation coefficient. All statistical analyses were performed with Prism 5 (ver. 5.04, GraphPad).

2. Parkinson's disease model

A. Animals

All animal studies were approved by the committee for the care and use of laboratory animals at Yonsei University College of Medicine. Six 6-OHDA unilaterally lesioned male Sprague-Dawley rats (420.85 ± 10.30 g, mean ± SD) and five control male Sprague-Dawley rats (383.38 ± 10.23 g, mean ± SD) were used for *in vivo* imaging of microPET. The rats were housed in a temperature and humidity controlled room with a 12 h light/dark cycle, and with free access to food and water.

B. Induce the hemi-Parkinson's model

The 6-OHDA is specifically uptake to the dopamine transporter (DAT) and noradrenalin transporter (NAT) from the extracellular membrane because 6-OHDA

is a hydroxylated analogue of the endogenous dopamine. In the intracellular space, 6-OHDA undergoes enzymatic degradation by monoamine oxidase-A (MAO-A) producing hydrogen peroxide, reactive oxygen species (ROS), and radicals as cytotoxic species. These cytotoxins cause neuronal damage[72]. In addition, 6-OHDA induces neurotoxicity by altering mitochondrial function[73]. In the animal model of PD, desmethylimiprimine (desipramine hydrochloride) was pretreated before administration of 6-OHDA to prevent uptake by noradrenergic terminals and to selectively destroy dopaminergic neurons.

Before anesthesia, the animals were pretreated with desipramine hydrochloride (12.5 mg/kg; intraperitoneal injection (i.p.), 12.5 mg/ml, 0.1 ml/100g). Surgery was performed under deep i.p ketamin/xylazine anesthesia (at dose of 40 mg/kg and 5 mg/kg, respectively). Each animal was positioned on a stereotaxic apparatus (Stoelting Co., Illinois, USA). The 20 μg/4 μl/site of 6-hydroxy dopamine (6-OHDA; Sigma-Aldrich, St. Louis, MO, USA) was injected into 2 sites (total of 40 μg 6-OHDA) in the right striatum according to the rat's brain atlas (Paxinos and Watson, 2007). 6-OHDA was injected into the following coordinates (relative to the bregma and dura): anterior-posterior (AP) + 0.5 mm, medial-lateral (ML) 2.5 mm, dorsal-ventral (DV) -5.0 mm & AP−0.5 mm, ML 4.2 mm, DV-5.0 mm at a rate of 1 μl/min using a 26G Hamilton syringe. The inserted needle was withdrawn from each location after 5 min, and skin was sutured.

C. Behavioral test

Rotational behavior was evaluated using a multichannel rotometer system (ROTORAT, MED Associates, Inc). Contralateral or ipsilateral rotational behaviors were induced by i.p. injection of d-amphetamine (5 mg/kg) on day 14 after the 6-OHDA injection. Each animal was placed in a cylindrical test chamber for 60 min. Counter-clockwise rotations were used for analysis. Animals showing more than 100 rotations per minute were considered successful and used for further experiments[74].

C. PET experiment & image analysis

Same procedure as Experiment II (Biological evaluation of [^{18}F]MEFWAY, p. 20).

D. Statistical analysis

All data were presented as mean ± standard error of the mean (SEM). The differences in BP_{ND} were analyzed with Student's unpaired t-test. All statistical analyses were performed with Prism 5 (ver. 5.04, GraphPad).

III. RESULTS

Experiment 1. Synthesis of [^{18}F]MEFWAY

1. An efficient synthesis of [^{18}F]MEFWAY precursor

WAY-100634 **(3**) was prepared as previously described[75] and total preparation steps of [^{18}F]MEFWAY precursor are described in Figure 5. Reaction of 2-aminopyridine with chloroacetyl chloride at room temperature provided 2-(chloroacetyl)amidopyridne (**1**) as an intermediate. The treatment of the intermediate with 1-(2-methoxy)piperzines in *N*,*N*-dimethylformamide (DMF) at 80^{o}C in the presence of K_2CO_3 and NaI gave the corresponding *N*-2-[2-{4-(2-methoxyphenyl)-1-piperazinyl}ethyl]amidopyridine (**2**), which was subsequently reduced to desired product **3**, using $LiAlH_4$ in tetrahydrofuran (THF) at room temperature.

The WAY-100634 was coupled with *trans*-4-carbomethoxycyclohexanecarbonyl chloride in dichloromethane in the presence of TEA at room temperature, yielding *trans*-*N*-2-{2-[4-(2-methoxy-phenyl)piperazinyl]ethyl}-*N*-(2-pyridyl)-*N*-(4-carboxymethylcyclohexane)carboxamide (**4**). In this reaction, I used oxalyl chloride

as a coupling agent instead of benzotriazole-1-yloxytris-(dimethylamino)-phophoniumhexafluoro-phosphate (BOP) to enhance the reactivity of carboxylic acid. This method improves the reaction yield up to 83%, more than twice the amount that was obtained using the previously reported method with BOP. Specific reduction of carbomethoxy group in **4** was conducted in $LiAlH_4$ in diethyl ether (Et_2O) at 0^oC to provide *trans*-*N*-2-{2-[4-(2-methoxyphenyl)piperazinyl]ethyl}-*N*-(2-pyridyl)-*N*-(4-hydroxymethylcyclo-hexane)carbox-amide (**5**) with a 57% yield. This new procedure dramatically improves the reaction yield compared to the previous protocol (<8% → 45%)[42].

For the preparation of the precursor **6**, the hydroxyl compound **5** was reacted with *p*-toluenesulfonyl anhydride to produce a 75% yield of the [^{18}F]MEFWAY precursor.

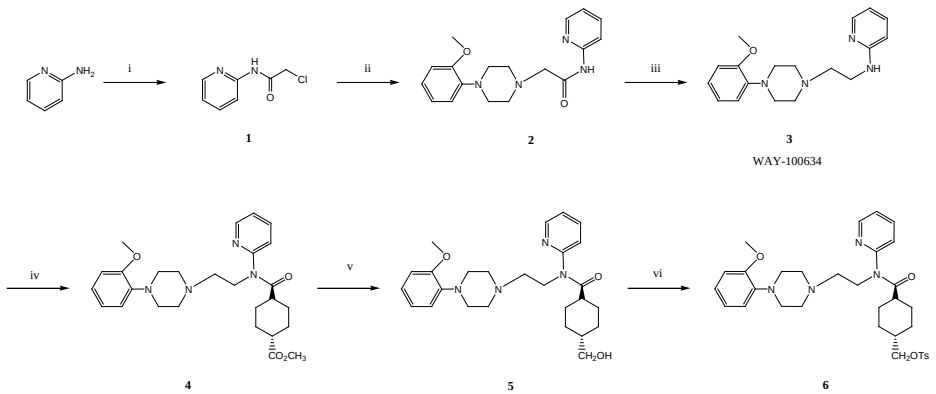

Figure 5. Synthetic scheme of [^{18}F]MEFWAY precursor. Reagents and conditions: i) choroacetyl chloride, TEA, CH_2Cl_2, r.t, 79%, ii) 1-(2-methoxyphenyl)-piperazine,

K_2CO_3, NaI, DMF, 80°C, 84%, iii) $LiAlH_4$, THF, r.t, 76%, iv) oxalylchloride, *trans*-4-carbomethoxycyclohexane-1-carboxylic acid, CH_2Cl_2, r.t, 83%, v) $LiAlH_4$, Et_2O, 0°C, 57%, vi) Ts_2O, TEA, CH_2Cl_2, r.t, 75% (r.t. = room temperature).

***N*-2-(2-chloroethyl)amidopyridine (1).** Chloroacetyl chloride (2.39 mL, 32.97 mmol) was slowly added to the mixture of 2-aminopyridine (1.88 g, 19.98 mmol) and TEA (4.30 mL, 30.69 mmol) in dry dichloromethane (100 mL) at 0°C. The reaction mixture was stirred at room temperature under an Argon atmosphere for 3 h. The organic layer was extracted with CH_2Cl_2, washed with water, and dried over anhydrous $MgSO_4$. The residue was purified by flash column chromatography (3:1 hexane/ethyl acetate) to give the product (2.68 g, 79%) as a white solid. ^{1}H NMR ($CDCl_3$, 300 MHz) δ 4.199 (s, 2H), 7.091-7.135 (m, 1H), 7.767-7.771 (m, 1H), 8.219-8.284 (m, 2H), 9.447 (s, 1H); ^{13}C NMR ($CDCl_3$, 75 MHz) δ 42.834, 114.327, 120.496, 139.113, 147.141, 150.383, 164.736; HRMS (FAB^+, *m*-nitrobenzylalcohol): Calcd. for $C_7H_8ON_2Cl$: 171.0325, Found: 171.0324.

***N*-2-[2-{4-(2-methoxyphenyl)-1-piperazinyl}ethyl]amidopyridine (2)** The mixture of 1-(2-methoxy)piperazine (0.20 mL, 1.17 mmol) and K_2CO_3 (0.40 g, 2.93 mmol) in DMF (8 mL) was stirred at 80°C for 1 h. After cooling down to room temperature, a solution of compound (1) (0.20 g, 1.17 mmol) in DMF (2 mL) and

sodium iodide (0.025 g, 0.17 mmol) were added to the mixture. The reaction mixture was stirred at 80^{o}C for 3 h, then cooled to room temperature. The organic layer was extracted with ethyl acetate, washed with water, and dried over anhydrous $MgSO_4$. The residue was purified by flash column chromatography (50:1 CH_2Cl_2/MeOH to 20:1 CH_2Cl_2/MeOH) to give the product (0.32 g, 84%) as a pale yellow oil. ^{1}H NMR ($CDCl_3$, 300 MHz) 2.819-2.850 (m, 4H), 3.179 (s, 4H), 3.244 (s, 2H), 3.870 (s, 3H), 6.859-7.055 (m, 5H), 7.688-7.747 (m, 1H), 8.251-8.325 (m, 2H), 9.639 (s, 1H); ^{13}C NMR ($CDCl_3$, 75 MHz) δ 50.635, 53.836, 55.386, 62.278, 111.209, 113.889, 118.354, 119.854, 121.013, 123.184, 138.332, 140.933, 147.985, 151.008, 152.254, 169.227; HRMS (FAB^{+}, *m*-nitrobenzylalcohol): Calcd. for $C_{18}H_{23}O_2N_4$: 327.1821, Found: 327.1818.

***N*-2-[2-{4-(2-methoxyphenyl)-1-piperazinyl}ethyl]-*N*-(2-pyridinyl)amine (3)**

1M LAH/THF (6.70 mL, 6.70 mmol) was slowly added to a solution of compound (2) (0.73 g, 2.24 mmol) in dry THF (10 mL) at 0^{o}C. The mixture was stirred at room temperature under an Argon atmosphere for 3 h. After quenching with saturated aqueous NH_4Cl at 0^{o}C for 30 min, the mixture was filtrated with ethyl acetate. The organic layer was extracted with ethyl acetate, washed with water, and dried over anhydrous $MgSO_4$. The residue was purified by flash column chromatography (50:1 CH_2Cl_2/MeOH to 20:1 CH_2Cl_2/MeOH) to give the product (0.53 g, 76%) as a pale yellow oil. ^{1}H NMR ($CDCl_3$, 300 MHz) δ 2.683-2.723 (m, 6H), 3.104 (s, 4H),

3.355-3.411 (m, 2H), 3.865 (s, 3H), 5.136 (s, 1H), 6.404-6.432 (d, 1H, J = 8.4 Hz), 6.541-6.585 (m, 1H), 6.848-7.036 (m, 4H), 7.388–7.446 (m, 1H), 8.083-8.108 (m, 1H); ^{13}C NMR ($CDCl_3$, 75 MHz) δ 38.515, 50.657, 53.119, 55.341, 56.759, 106.987, 111.126, 112.660, 118.198, 120.972, 122.917, 137.300, 141.300, 148.201, 152.253, 158.827; HRMS (FAB^+, *m*-nitrobenzylalcohol): Calcd. for $C_{18}H_{25}ON_4$: 313.2028, Found: 313.2030.

***trans*-*N*-2-[2-{4-(2-methoxyphenyl)piperazinyl}ethyl]-*N*-(2-pyridyl)-*N*-(4-carboxymethylcyclohexane)carboxamide (4)** Oxalylchloride (0.19 mL, 2.13 mmol) was added to a solution of *trans*-4-carbomethoxycyclohexane-1-carboxylic acid (0.20 g, 1.05 mmol) in dry CH_2Cl_2 (10 mL), and the mixture was refluxed for 2 h. After removing the solvent and unreacted oxalylchloride under reduced pressure, the product was re-dissolved in dry CH_2Cl_2. Compound (3) (0.22 g, 1.05 mmol) and TEA (0.16 mL, 1.14 mmol) were added to the previous product at 0^{o}C. The reaction mixture was stirred at room temperature under an Argon atmosphere for 2 h. After the mixture was washed with 10% aqueous $NaHCO_3$ (100 mL), the organic layer was extracted with CH_2Cl_2, and dried over anhydrous $MgSO_4$. The residue was purified by flash column chromatography (ethyl acetate, 0.1 % v/v TEA) to give the product (0.28 g, 83%) as a pale yellow oil. ^{1}H NMR ($CDCl_3$, 300 MHz) δ 1.166-1.250 (m, 2H), 1.615-1.660 (m, 2H), 1.839-1.962 (m, 4H), 2.252-2.292 (m, 2H), 2.581-2.626 (m, 6H), 2.983 (s, 4H), 3.617 (s, 3H), 3.840 (s, 3H), 3.951-3.997 (m,

2H), 6.828-6.997 (m, 4H), 7.237-7.307 (m, 2H), 7.739-7.797 (m, 1H), 8.514-8.534 (m, 1H); ^{13}C NMR ($CDCl_3$, 75 MHz) δ 27.812, 28.267, 41.311, 42.094, 44.794, 50.062, 51.374, 52.986, 55.155, 55.642, 110.981, 117.924, 120.749, 121.922, 122.357, 122.791, 138.249, 140.880, 149.171, 151.994, 175.459, 175.996; HRMS (FAB^+, *m*-nitrobenzylalcohol): Calcd. for $C_{27}H_{37}O_4N_4$: 481.2815, Found: 481.2814.

***trans*-*N*-2-[2-{4-(2-methoxyphenyl)piperazinyl}ethyl]-*N*-(2-pyridyl)-*N*-(4-hydroxymethylcyclohexane)carboxamide (5)** 1M LAH/diethyl ether (0.16 mL, 0.16 mmol) was slowly added to the solution of compound (4) (0.076 g, 0.16 mmol) in diethyl ether (5 mL) at 0^{o}C. The reaction mixture was stirred for 30 min at 0^{o}C under an Argon atmosphere, and quenched with saturated aqueous NH_4Cl. The organic layer was extracted with ethyl ether, and then the solvent was evaporated under reduced pressure. The residue was purified by gravity column chromatography using neutral silica gel (30 : 1 CH_2Cl_2/MeOH) to give the product (0.041 g , 57 %) as a colorless oil. ^{1}H NMR ($CDCl_3$, 300 MHz) δ 1.578-1.852 (10H, m), 2.588-2.634 (m, 6H), 2.981 (s, 4H), 3.369-3.389 (d, 2H, *J* = 6.0 Hz), 3.837 (s, 3H), 3.961-4.007 (t, 2H, *J* = 6.9 Hz), 6.826-6.982 (m, 4H), 7.222-7.280 (m, 2H), 7.738-7.763 (m, 1H), 8.513-8.534 (m, 1H); ^{13}C NMR ($CDCl_3$, 75 MHz) δ 28.437, 28.875, 39.568, 42.333, 45.202, 50.564, 53.334, 55.307, 56.135, 68.316, 111.130, 118.058, 120.894, 122.250, 122.822, 138.146, 141.271, 149.277, 152.196, 155.829,

176.023; HRMS (FAB$^+$, *m*-nitrobenzylalcohol): Calcd. for $C_{26}H_{37}O_3N_4$: 453.2866, Found: 453.2870.

***trans*-*N*-2-[2-{4-(2-methoxyphenyl)piperazinyl}ethyl]-*N*-(2-pyridyl)-*N*-(4-tosyloxymethylcyclohexane)carboxamide (6)** *p*-toluenesulfonyl anhydride (0.018 g, 0.056 mmol) and TEA (0.0072 mL, 0.050 mmol) were added to the solution of compound (5) (0.021 g, 0.046 mmol) in CH_2Cl_2 (5 mL). The reaction mixture was stirred at room temperature under an Argon atmosphere for 48 h. After the mixture was washed with 10% aqueous $NaHCO_3$ (100 mL), the organic layer was extracted with CH_2Cl_2, and dried over anhydrous $MgSO_4$. The residue was purified by gravity column chromatography using neutral silica gel (20 : 1 CH_2Cl_2/MeOH) to give the product (0.022 g , 75 %) as a colorless oil. ^{1}H NMR ($CDCl_3$, 300 MHz) δ 1.252-1.779 (m, 10H), 2.436 (s, 3H), 2.567-2.612 (m, 6H), 2.973 (s, 4H), 3.740-3.759 (d, 2H, *J* = 9.5 Hz), 3.836 (s, 3H), 3.960-3.983 (t, 2H, *J* = 6.9 Hz), 6.826-6.955 (m, 4H), 7.248-7.330 (m, 4H), 7.722-7.765 (m, 3H), 8.507-8.527 (m, 1H); ^{13}C NMR ($CDCl_3$, 75 MHz) δ 21.631, 27.988, 28.507, 36.374, 41.847, 45.280, 50.597, 53.350, 55.313, 56.121, 74.890, 111.139, 118.056, 120.905, 122.173, 122.372, 122.826, 127.831, 129.793, 132.945, 138.243, 141.282, 144.675, 149.326, 152.205, 155.765, 175.627; HRMS (FAB$^+$, *m*-nitrobenzylalcohol): Calcd. for $C_{33}H_{43}O_5N_4S$: 607.2954, Found: 607.2954.

2. Synthesis of non-radioactive MEFWAY and WAY-100635

A. Preparation of non-radioactive MEFWAY (standard MEFWAY)

Diethylaminosulfur trifluoride (DAST) (0.047 mL, 0.32 mmol) was added drop-wise to the solution of *trans*-*N*-2-{2-[4-(2-methoxyphenyl)piperazinyl]ethyl}-*N*-(2-pyridyl)-*N*-(4-hydroxymethylcyclohexane)carboxamide (5) (0.074 g, 0.16 mmol) in CH_2Cl_2 (10mL) at 0^oC under Argon atmosphere. The mixture was allowed to warm to room temperature and stirred for 24 h. After reaction, the mixture was quenched by the addition of 10% $NaHCO_3$ (0.5 mL) and the organic layer was extracted with CH_2Cl_2 followed by drying over anhydrous $MgSO_4$. The crude product was purified by HPLC (a preparative reverse phase C-18 column, acetonitrile: H_2O containing 0.1% TEA, flow rate 5 mL/min, retention time = 12.3 min). The solvent was evaporated under reduced pressure to give the product (0.032 g, 45 %) as a colorless oil. ^{1}H NMR ($CDCl_3$, 300 MHz) δ 0.731-0.806 (m, 2H), 1.505-1.791 (m, 7H), 2.130 (s, 1H), 2.525-2.552 (m, 6H), 2.910 (s, 4H), 3.763 (s, 3H), 3.899-3.926 (t, 2H, *J* = 6.9 Hz), 4.030-4.041 (d, 1H, *J* = 5.6 Hz), 4.125-4.136 (d, 1H, *J* = 5.5 Hz), 6.760-6.921 (m, 4H), 7.155-7.236 (m, 2H), 7.669-7.703 (t, 1H, *J* = 5.9 Hz), 8.445-8.457 (d, 1H, *J* = 3.4 Hz).^{13}C NMR ($CDCl_3$, 75 MHz) δ 27.671, 28.852, 29.858, 37.946, 42.315, 45.459, 50.813, 53.573, 55.531, 56.408, 87.734, 89.071, 111.512, 118.266,

121.141, 122.372, 122.412, 122.963, 138.293, 141.592, 149.458, 152.463, 156.096, 176.025; HRMS (FAB^+, *m*-nitrobenzylalcohol): Calcd. for $C_{26}H_{36}O_2N_4F$: 455.2822, Found: 455.2820.

B. Preparation of non-radioactive WAY-100635

Oxalylchloride (0.52 mL, 5.82 mmol) was added to a solution of cyclohexanecarboxylic acid (0.37 mL, 2.91 mmol) in dry CH_2Cl_2 (10 mL), and the mixture was refluxed for 2 h. After removing the solvent and unreacted oxalylchloride under reduced pressure, the product was re-dissolved in dry CH_2Cl_2. Compound (3) (0.65 g, 2.08 mmol) and TEA (0.44 mL, 3.12 mmol) were added to the previous product at 0^oC. The reaction mixture was stirred at room temperature under an Argon atmosphere for 2 h. After the mixture was washed with 10% aqueous $NaHCO_3$ (100 mL), the organic layer was extracted with CH_2Cl_2, and dried over anhydrous $MgSO_4$. The residue was purified by flash column chromatography (ethyl acetate, 0.1 % v/v TEA) to give the product (0.66 g, 75%) as a pale yellow oil. ^1H NMR ($CDCl_3$, 300 MHz) δ 0.920-0.972 (m, 2H), 1.104-1.143 (m, 1H), 1.427-1.509 (m, 3H), 1.604-1.688 (m, 4H), 2.171(s, 1H), 2.530-2.558 (m, 6H), 2.912 (s, 4H), 3.761 (s, 3H), 3.905-3.932 (t, 2H, *J* = 6.9 Hz), 6.758-6.919 (m, 4H), 7.141-7.231 (m, 2H), 7.659-7.693 (m, 1H), 8.442-8.454 (d, 1H, *J* = 3.4 Hz); ^{13}C NMR

($CDCl_3$, 75 MHz) δ 25.846, 29.702, 42.561, 45.305, 50.761, 53.537, 55.506, 56.427, 111.470, 118.249, 121.114, 122.239, 122.435, 122.933, 138.143, 141.562, 149.365, 152.430, 156.153, 176.414; HRMS (FAB^+, *m*-nitrobenzylalcohol): Calcd. for $C_{25}H_{35}O_2N_4$: 423.2760, Found: 423.2756.

3. Radiosynthesis of [^{18}F]MEFWAY

A. Production of K222-K[^{18}F]F complex

$^{18}F^-$ was produced by the $^{18}O(p,n)^{18}F$ reaction using enriched [^{18}O]water in the cyclotron. At the end of bombardment, the $^{18}F^-/H_2{}^{18}O$ was transferred with helium pressure to the reaction vial in lead-shielded hot-cells.

The first step is to remove bulk [^{18}O]water. This is achieved by adsorption of [^{18}F]fluoride ion into a QMA, which was preconditioned with 5 mL of 1M K_2CO_3 followed by 5 mL of water. Then, F-18 was extracted with an eluent, which is composed of K222 (22mg) in acetonitrile (0.9ml) and K_2CO_3 (1mg) in H_2O (0.1ml). The residual water was evaporated under a stream of nitrogen at 100^{o}C and co-evaporated with acetonitrile (0.5 mL x 3). The dried fluorinating agent K222-K[^{18}F]F was then used for radiosynthesis.

B. Radiosynthesis and purification of [^{18}F]MEFWAY

[^{18}F]MEFWAY was synthesized according to the procedure previously described[42]. The *trans*-tosylated precursor was reacted with the dried K222-K[^{18}F] complex in acetonitrile at 105^{o}C for 15 min. In this step, the radiolabeling yield was 79% (Figure 6A). Purification by semi-preparative HPLC gave a solution of [^{18}F]MEFWAY in acetonitrile/water containing 0.1% TEA (Figure 6B). After diluting with distilled water, the solution was passed through a C-18 Sep-Pak Light cartridge. The cartridge was further washed with water to remove traces of organic solvents, and the product was extracted with 1 mL of ethanol. Finally, the ethanol was diluted with 10 mL of isotonic saline solution and sterile-filtered through a 0.22 μm membrane filter for intravenous application. The identity of the formulated [^{18}F]MEFWAY was confirmed by co-injecting standard MEFWAY (Figure 6D). The total synthesis time was 54 ± 10 min (n = 45). The radiochemical purity of [^{18}F]MEFWAY used in this study was greater than 99% (Figure 6C) and the specific activity ranged between 87.4-108.2 GBq/μmol at the end of synthesis.

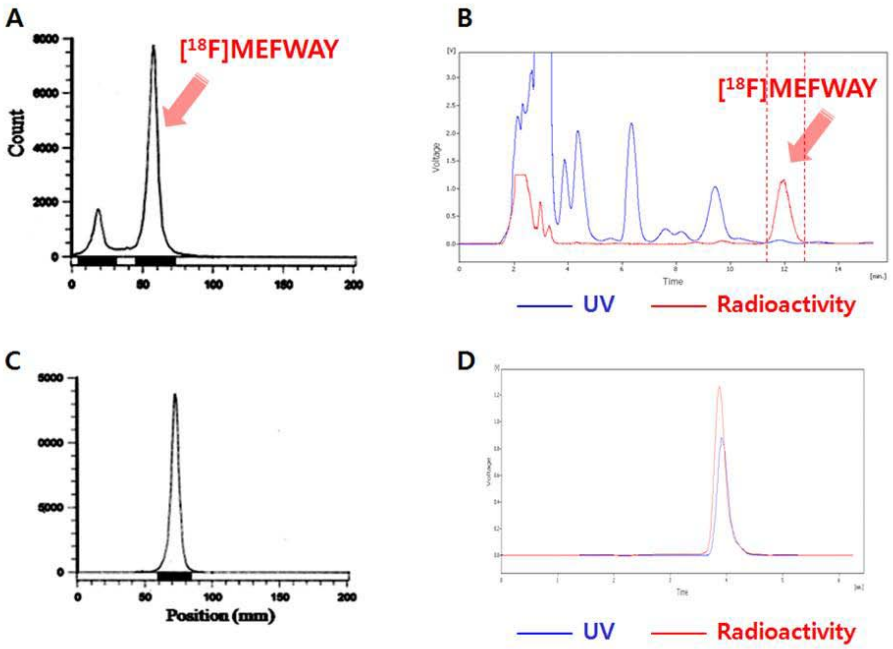

Figure 6. Confirmation and analysis of [^{18}F]MEFWAY following radiosynthesis. (A) After incorporating radioactive F-18 into *trans*-tosylated precursor, crude [^{18}F]MEFWAY (red arrow) was obtained with a radiolabeling yield of 79% based on starting F-18. Left peak corresponds to un-reacted free F-18 anions. (B) Then, the crude product was purified using HPLC (blue line corresponds to UV signal and red line means radioactivity signal). The [^{18}F]MEFWAY that fell between the dotted lines (11.6-12.7 min) was collected. (C) The radiochemical purity of final [^{18}F]MEFWAY was checked (>99%). (D) Finally, the identity of [^{18}F]MEFWAY was confirmed using co-injection of non-radioactive MEFWAY.

4. Quality control of [^{18}F]MEFWAY

The product was obtained as a sterile solution ready for the intravenous injection and as a colorless solution without any precipitates. pH by pH strip showed the around 7. Radiochemical purity exceeded 99% as determined by radio-TLC and radiochemical identity by the relative retention time to reference MEFWAY was 1.01. Residual solvents as determined by GC were found to be acetonitrile < 400 ppm acetonitrile. Radionuclidic purity by MCA was appeared at 511 MeV. Concentration of endotoxins was found to be below 1.01 EU/mL and all samples passed the test for sterility. Concluding, all quality control parameters were in accordance with the standard for parenteral animal application.

Table 3. Quality control parameters in the final [^{18}F]MEFWAY.

	Release criteria	Result
Visual inspection	Clear, no ppt	Pass
pH	4.5-7.5	7.0
Radiochemical purity	≥ 95%	≥99 %
Radiochemical Identity	RRT = 0.9 - 1.1	1.01
Residual solvent analysis	<400 ppm for acetonitirle	60 ppm
Radionuclidic purity	511 or 1022 KeV	pass
Endotoxin	<25.0 EU/mL	Pass

Experiment 2. The efficacy of [^{18}F]MEFWAY *in vivo*

1. Metabolic stability of [^{18}F]MEFWAY

Although [^{18}F]MEFWAY was developed to complement *in vivo* defluorination of [^{18}F]FCWAY, there is no report about its *in vivo* stability against defluorination. To evaluate the metabolic stability of [^{18}F]MEFWAY, authentic [^{18}F]MEFWAY PET images were obtained from the rats (control group). In this case, the skull uptake of radioactivity continuously increased and reached 7.17 SUV at 105 min soon after injection (Figure 7-8).

It is known that defluorination of [^{18}F]FCWAY is due to the CYP450 in the liver and this enzyme can be suppressed by antifungal drugs such as miconazole or fluconazole. To assess the inhibitory activity of miconazole and fluconazole to [^{18}F]MEFWAY metabolism, rats were pretreated with 10, 30, and 60 mg/kg miconazole or fluconazole prior to the administration of [^{18}F]MEFWAY. PET images revealed that the skull uptake of radioactivity decreased in a dose-dependent manner. Radioactivities in the skull at 105 min were 7.17, 4.32, 2.69, and 1.36 SUV with increasing fluconazole pretreatment, and 7.17, 5.44, 2.77, and 2.20 SUV with increasing miconazole pretreatment (Figure 7). As such, fluconazole (60 mg/kg intravenously) effectively suppressed the skull uptake by 81% compared to control.

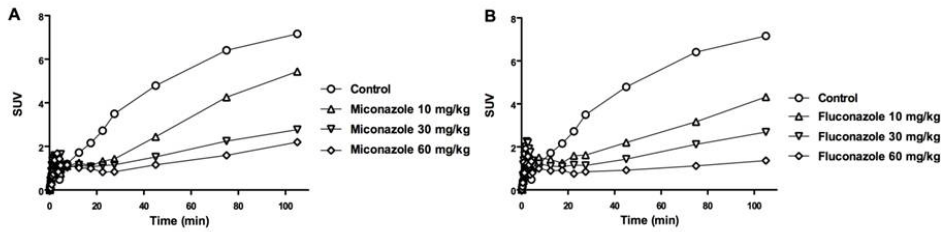

Figure 7. Time-activity curves of [^{18}F]MEFWAY uptake in skull for control and various dosages of inhibitors, fluconazole and miconazole. (A) Pretreatment of miconazole, control (○), miconazole 10 mg/kg (▵), miconazole 30 mg/kg (▿), miconazole 60 mg/kg (◇), (B) Pretreatment of fluconazole, control (○), fluconazole 10 mg/kg (▵), fluconazole 30 mg/kg (▿), fluconazole 60 mg/kg (◇). Skull uptake of control [^{18}F]MEFWAY was increased over time. This uptake was suppressed by the pretreatment of miconazole or fluconazole in a dose-dependent manner. At the highest dose, fluconazole was more potent than miconazole.

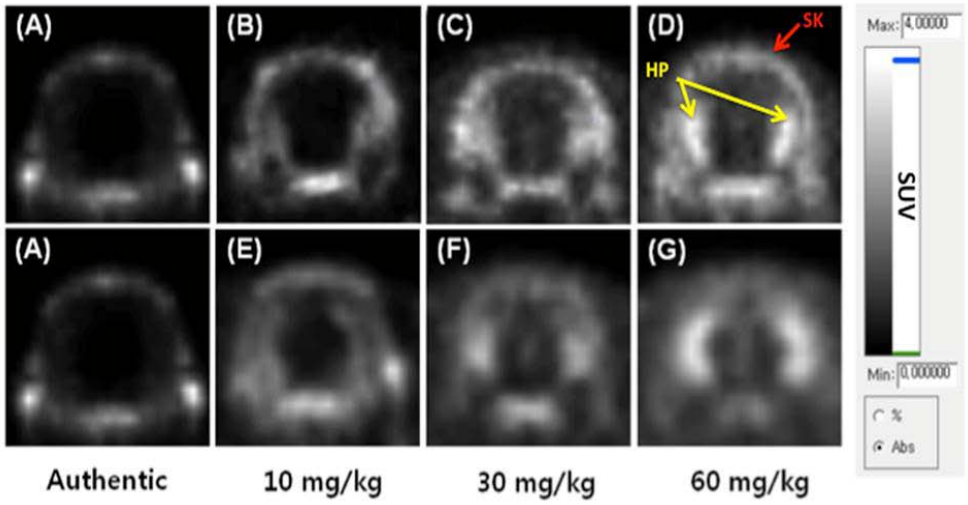

Figure 8. PET images of [^{18}F]MEFWAY uptake in skull and brain for control and various dosages of inhibitors, fluconazole and miconazole. PET images of the brain acquired between 60 and 90 min after administration of [^{18}F]MEFWAY. HP: hippocampus, SK: skull, (A) Authentic [^{18}F]MEFWAY (no treatment), (B) Miconazole (10 mg/kg), (C) Miconazole (30 mg/kg), (D) Miconazole (60 mg/kg), (E) Fluconazole (10 mg/kg), (F) Fluconazole (30 mg/kg) and (G) Fluconazole (60 mg/kg). Radioactivity of authentic [^{18}F]MEFWAY was predominantly uptaken to the skull. By increasing the dosage of miconazole and fluconazole, this skull uptake was diminished, whereas hippocampal uptake was increased.

I thought that as the inhibition of defluorination using fluconazole increased, the brain uptake would correspondingly increase as the non-metabolized

[^{18}F]MEFWAY is uptake to the brain. To confirm this, I analyzed the brain uptakes using various dosages of fluconazole.

In the control [^{18}F]MEFWAY, regional time-activity curves exhibited a moderate uptake of radioactivity into 5-HT_{1A} receptor-rich regions (frontal cortex and hippocampus) followed by a slow clearance of radioactivity. In the 5-HT_{1A} receptor-poor cerebellum, radioactivity showed a fast uptake and a rapid washout pattern (Figure 9A).

Radioactivity in the cerebellum was generally similar to the control over time (Figure 9A-D). PET images showed the highest uptake of radioactivity in the HP and FC over 75 min at 60 mg/kg of fluconazole. After rats were pretreated with 10, 30, and 60 mg/kg fluconazole prior to the administration of [^{18}F]MEFWAY, the ratio of radioactivity in HP or FC to that of the skull successively increased from 0.26 to 2.72 SUV and from 0.20 to 1.52 SUV, respectively.

These results suggested that defluorination of [^{18}F]MEFWAY can be effectively suppressed by fluconazole allowing for the quantification of 5-HT_{1A} receptor density.

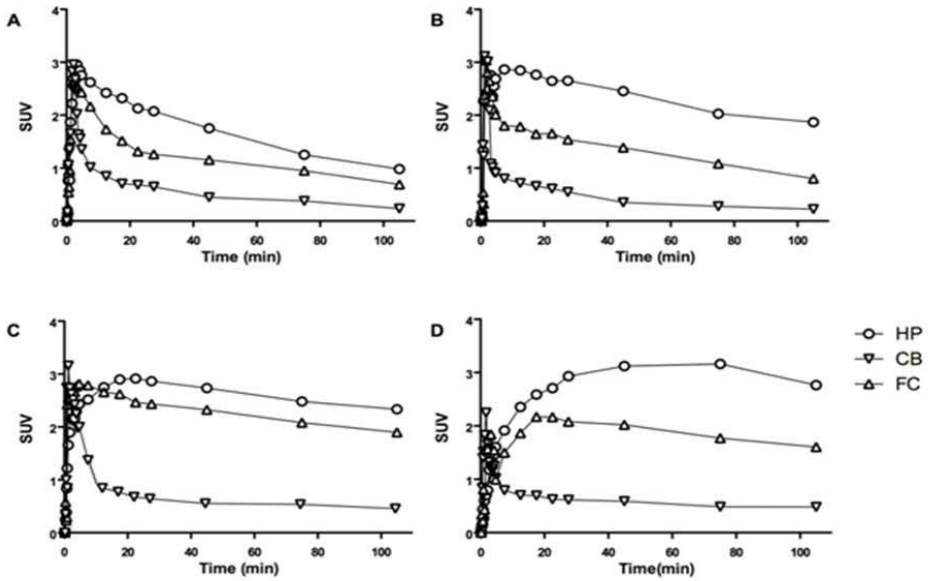

Figure 9. Time-activity curves of [^{18}F]MEFWAY in specific brain regions for various dosages of fluconazole. Hippocampus (HP, ○), frontal cortex (FC, ▵), and cerebellum (CB, ▿). Rats were pretreated with various dosages of fluconazole before administration of [^{18}F]MEFWAY. Fluconazole dose: (A) 0 mg/kg (control), (B) 10 mg/kg, (C) 30 mg/kg, (D) 60 mg/kg. As the dosage of fluconazole was increased, radioactivities in the hippocampus and frontal cortex were increased whereas cerebellar uptakes were generally similar to the control.

Time-activity curves of specific binding (SUV_{ROI} - SUV_{CB}, ROI of FC or HC) to non-specific binding (SUV_{CB}) were shown in Figure 10. The binding potential (BP)

in PET research has been used to estimate the available number of receptors. In addition, differences in BP indicate the up- or down-regulation of the receptors. Non-displaceable binding potential (BP_{ND}) was determined by using the transient equilibrium method, which is the ratio of peak value of the specific binding curve divided by non-specific curve (i.e. cerebellar curve). The BP_{ND} values in the HP and FC were 5.53 and 2.66 at 75 min. Optimal acquisition time for the quantification of 5-HT_{1A} receptor using [^{18}F]MEFWAY is 75-110 min because this time window has maximal value of specific to non-specific ratio.

This result suggested that [^{18}F]MEFWAY has a high target-to-nontarget ratio.

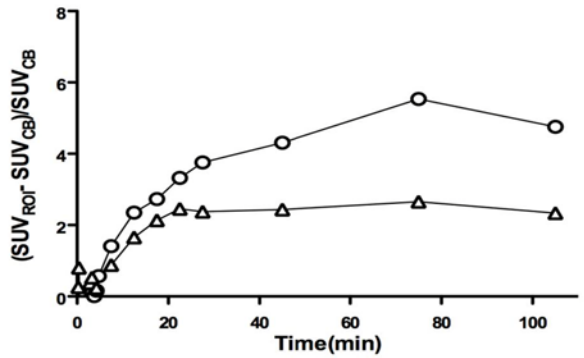

Figure 10. Ratio of [^{18}F]MEFWAY specific to non-specific binding curves in the hippocampus. (SUV_{HP}-SUV_{CB})/SUV_{CB} (○), (SUV_{FC}-SUV_{CB})/SUV_{CB} (△). The peak ratios of specific to non-specific binding in the hippocampus and frontal cortex reached about 5.53 and 2.66 at 75 min, respectively.

2. Specificity of [^{18}F]MEFWAY to 5-HT$_{1A}$ receptors

To confirm the specificity of [^{18}F]MEFWAY to 5-HT$_{1A}$ receptors, pre-block and displacement experiments were performed with a highly specific antagonist for 5-HT$_{1A}$ receptor. In the pre-block experiment in which 1.5 mg/kg of non-radioactive WAY-100635 was administrated before the injection of [^{18}F]MEFWAY, radioactivity was remarkably reduced by 88% in total binding in the whole brain at about 10 min (Figure 11A). In the displacement experiment in which 1.5 mg/kg of non-radioactive WAY-100635 was administered at 30 min after injection of [^{18}F]MEFWAY, the radioactivity in the 5-HT$_{1A}$-receptor-rich HP decreased immediately, resulting in hippocampal uptake of less than 1.2 SUV at 120 min (Figure 11B). This result suggested that [^{18}F]MEFWAY is a specific PET radioligand to the 5-HT$_{1A}$ receptors.

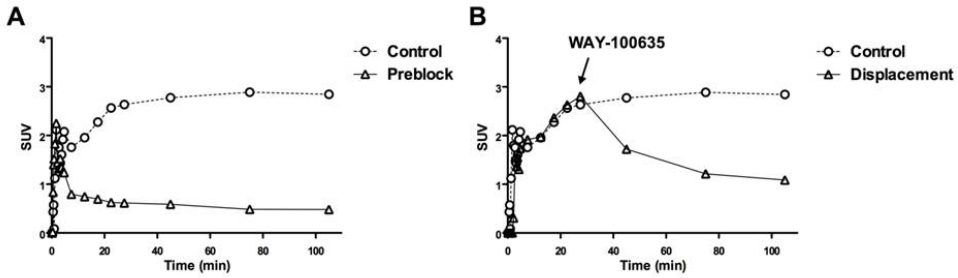

Figure 11. Pre-block and displacement experiments with non-radioactive WAY-100635. (A) Pre-block experiment with non-radioactive WAY-100635, control (○), pre-block (▵) and (B) Displacement experiments of [^{18}F]MEFWAY with non-radioactive WAY-100635, control (○), displacement (▵). In 5-HT$_{1A}$ receptors pre-blocked with non-radioactive WAY-100635, [^{18}F]MEFWAY showed fast washout pattern in the whole brain. Whereas, interim administration of WAY-100635 caused immediately decreasing radioactivity in the hippocampus.

Experiment III. Application to animal disease models

1. Acute model for depression

Forced swimming stress is used to evoke the acute model for depression. *In vitro* binding assay indicated that this powerful stimuli causes the down-regulation of 5-HT_{1A} receptors in the hippocampus[76]. However, no research has been conducted in the living animal so far. I investigated whether [^{18}F]MEFWAY is an applicable PET radioligand in a live acute model for depression. In order to evoke this model, rats were exposed to forced swimming. In this situation, rats will immediately struggle for a period of time and then eventually become immobile (immobility, behavioral despair). I performed the [^{18}F]MEFWAY PET experiment in the control and forced swimming groups (despair group).

As a result, representative summed PET images of [^{18}F]MEFWAY displayed a significant reduction of hippocampal uptake in the despair group (Figure 12). The hippocampal uptake in the despair group was about 25% lower than that of control group (Figure 13A). The ratio of specific binding to the non-specific binding in the despair group was 18% lower than that of control (Figure 13B).

To compare the change in the 5-HT_{1A} receptor density in the hippocampus of despair to the control group, I obtained the BP_{ND}. The BP_{ND} in the despair group was decreased by 18% compared with the control (Figure 14).

I hypothesized that the greater the despair in the rat, the greater the reduction in available 5-HT_{1A} receptors in the hippocampus would be. The duration time of the immobility indicates the despair severity and the BP_{ND} represents the availability of the receptors in the plasma membrane. In order to figure out the relationship between BP_{ND} and immobility, I analyzed the individual PET data and behavioral test.

The BP_{ND} and the immobility in the despair group were negatively correlated (Figure 15) and showed a strong correlation with a statistically significant difference (R^2 = 0.80, P = 0.0027). These data suggest that [^{18}F]MEFWAY can detect the change of the 5-HT_{1A} receptor density in an acute model for depression.

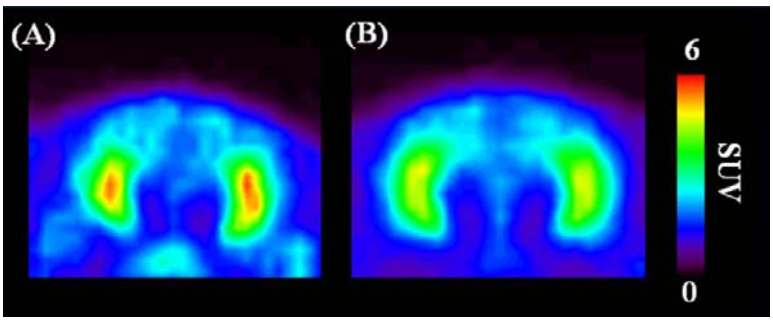

Figure 12. Representative PET images of [^{18}F]MEFWAY in the control and the forced swimming stressed rat. Control (A), and the despair group (B). Hippocampal uptake in despair group was significantly lower than in the control group.

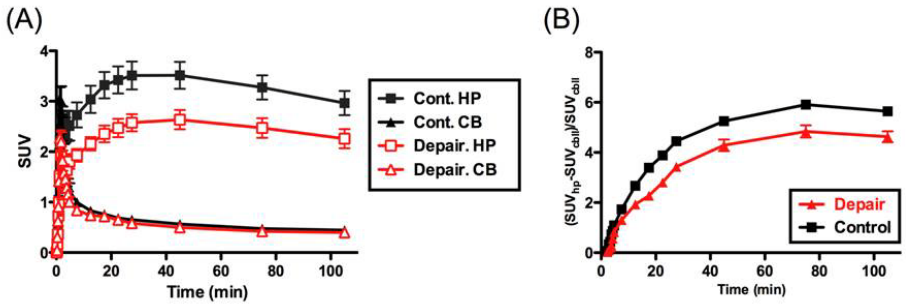

Figure 13. Time-activity curves of [^{18}F]MEFWAY uptake in specific regions of the brain for the control and the forced swimming stress group (despair group). (A) Control hippocampus (Cont. HP, ■), control cerebellum (Cont. CB, ▲), despair hippocampus (Despair. HP, ▫) and despair cerebellum (▵). In despair group, hippocampal uptake was 20% lower than in the control while cerebellar uptake was almost the same as in control. (B) Control (■), despair group (▲). The ratio of specific to non-specific binding in despair group was 18% lower than in the control. Data represent mean ± SEM values for eight independent experiments in the control and for seven independent experiments in the despair group.

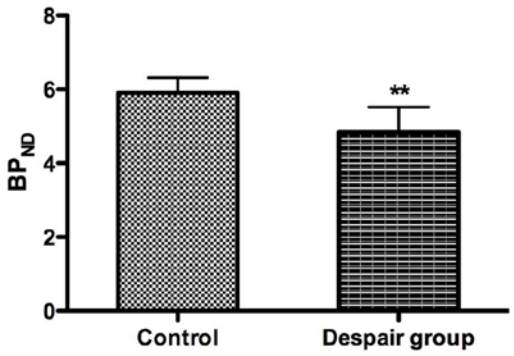

Figure 14. Comparison of the BP_{ND} of [^{18}F]MEFWAY in the hippocampus between the control and the forced swimming stress group (despair group). Mean (±SEM) bars indicate the significant differences in the BP_{ND} ($^{*}P$ = 0.0032) compared with the control. Data represent mean ± SEM values for eight independent experiments in the control and for seven independent experiments in the despair group. Statistical significance was determined using a Student's unpaired t-test.

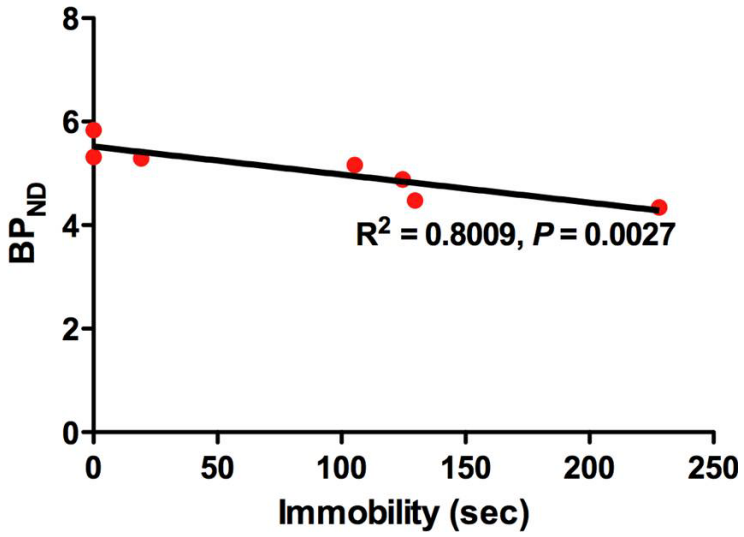

Figure 15. Correlation between [^{18}F]MEFWAY BP_{ND} in the hippocampus and immobility in the forced swimming stress group (despair group). This graph showed that BP_{ND} and immobility in the despair group were negatively correlated. The coefficient of the determination (R^2) of 0.80 indicates high correlation between BP_{ND} and immobility.

2. Parkinson's disease model

Unilateral 6-OHDA lesion is used to make a hemi-Parkinsonian model. This 6-OHDA selectively destroys the presynaptic nerve endings of dopaminergic neurons. Previous researches suggest that the degeneration of the dopaminergic system cause the alteration of serotonergic system. However, there is no direct evidence for the alteration of the 5-HT_{1A} receptor density in the limbic system. Recently, it was shown that an unilateral 6-OHDA lesion in rats induced the bilateral reduction of the 5-HT_{2A} receptor density in cortical area[77]. This result implied that the unilateral degeneration of dopaminergic neurons might influence the 5-HT_{1A} receptor density in the limbic system. To investigate the effect of the 6-OHDA lesion, I performed the [^{18}F]MEFWAY PET experiment in the control and 6-OHDA lesion groups.

In 6-OHDA lesioned rats, a severe reduction of radioactivity in hippocampus appeared (Figure 16B). Interestingly, the hippocampal uptake of 6-OHDA lesioned rats was about 39% lower than that of the control group and the symmetry of radioactivity in both left and right hippocampuses was preserved (Figure 17A). In addition, the ratio of specific binding to non-specific binding in the 6-OHDA group was 27% lower than that of the control group (Figure 17B).

To compare the change in the 5-HT_{1A} receptor density in the hippocampuses of 6-OHDA group and the control, I obtained the BP_{ND}. The BP_{ND} in the 6-OHDA group decreased by 30% compared with the control group (Figure 18).

These data suggest that [^{18}F]MEFWAY can detect the change of the 5-HT$_{1A}$ receptor density in a hemi-Parkinsonian model.

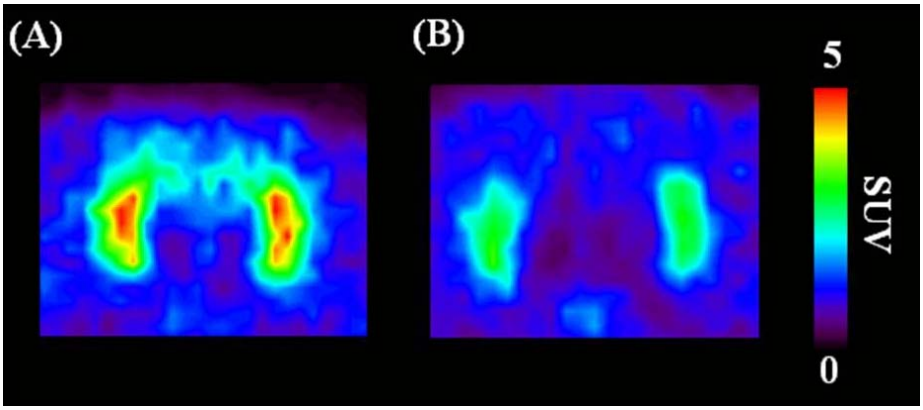

Figure 16. Representative PET images of [^{18}F]MEFWAY in the control and the 6-OHDA lesioned rat. Control (A) and unilateral 6-OHDA lesion rat (B). Hippocampal uptake in 6-OHDA lesioned model was significantly lower than in control group.

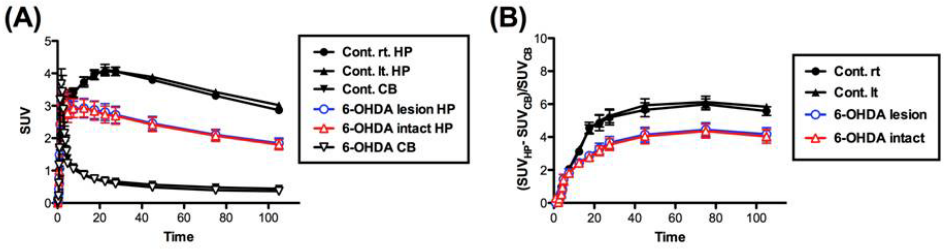

Figure 17. Time-activity curves of [^{18}F]MEFWAY uptake in the specific regions of the brain for the control and the 6-OHDA lesion group. (A) Control right

hippocampus (Cont. rt. HP, •), control left hippocampus (Cont. lt. HP, ▲), control cerebellum (Cont. CB, ▼), 6-OHDA lesion hippocampus (6-OHDA lesion HP, ○), 6-OHDA intact hippocampus (6-OHDA intact HP, △), 6-OHDA cerebellum (6-OHDA CB, ▽). In 6-OHDA rats, hippocampal uptake was 39% lower than in control while cerebellar uptake was similar to control. (B) Control right (•), Control left (▲), 6-OHDA lesion (○), 6-OHDA intact (△). The ratio of specific to non-specific binding in 6-OHDA rats was 27% lower compared with control. Data represent mean ± SEM values for five independent experiments.

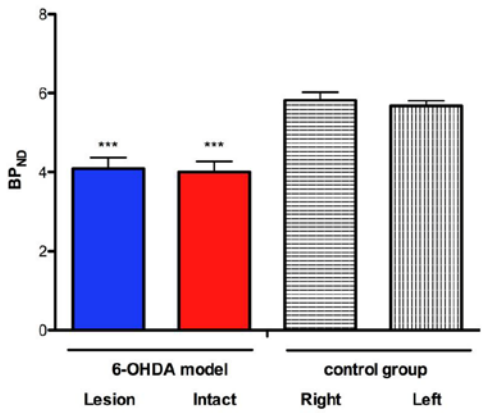

Figure 18. Comparison of [^{18}F]MEFWAY BP_{ND} in the hippocampus between the 6-OHDA lesion and the control group. Mean (±SEM) bars indicate the significant differences in the lesion site ($^{***}P$ = 0.0004) compared with right region of control, and intact site ($^{***}P$ = 0.004) compared with left region of control. However, there were no significant differences between the lesion and intact site (P = 0.819). Data

represent mean ± SEM values for four independent experiments. Statistical significance was determined using a Student's unpaired t-test.

IV. DISCUSSION

1. Synthesis of [^{18}F]MEFWAY precursor

Although [^{18}F]MEFWAY had been developed, the synthetic method of its precursor was inefficient with a low overall yield (<8%). Therefore, there is a need for improvement of this synthetic yield. The major problems of the reported method were the use of an improper coupling agent (i.e. BOP) and significant breakdown of the amide bond.

The coupling ability of BOP-based intermidiate to the WAY-100634 is poorer than that of the acid chloride (i.e. oxalyl chloride) because BOP is too bulky to readily react with the secondary amine[78](Figure 19).

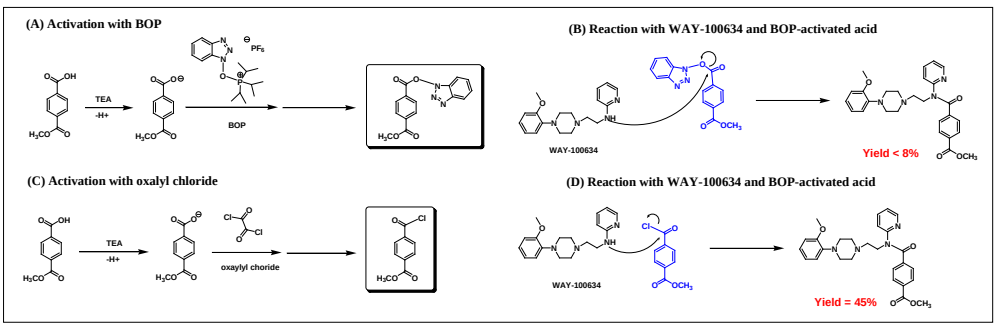

Figure 19. Comparison of reaction mechanisms between BOP and oxalyl choride based reaction. The reaction intermidate from the BOP (A) is too bulky to react with

the substrate (i.e. WAY-100634)(B), whereas the intermidate from the oxalyl chloride (C) relatively easily reacts with the substrate (D).

In the specific reduction step of methyl ester bond to the primary alcohol, $LiAlH_4$/THF facilitated significant breakdown of the amide bond to yield WAY-100634 (i.e. up to 70% of starting substrate) due to the possible presence of unusual reactivity of $LiAlH_4$ in solution of THF or adventitious water in THF. $LiAlH_4$ reacts violently with water molecules to produce hydrogen gas. Therefore it should not be exposed to moisture and the reaction must be carried out in anhydrous non-protic solvents like THF and diethyl ether.

It is well known that although THF has lower solubility than diethyl ether for $LiAlH_4$, THF is preferred over diethyl ether due to the stability of $LiAlH_4$ (solubility for $LiAlH_4$ at 25^{o}C: diethyl ether 5.92 mol/L and THF 2.96 mol/L). In this case, however, $LiAlH_4$/diethyl ether is more suitable than $LiAlH_4$/THF because the former reduction system has a faster reaction rate than the later system. Due to the fast reaction rate of LAH/diethyl ether, the alcohol product is a major component and the starting material, an ester compound, is a minor compound.

Chemoselectivity means the selective reactivity of one functional group in the presence of others. In case of synthetic method of the MEFWAY, the compound (4) has two kinds of carbonyl groups that each form an amide bond and an ester bond. The most important reducing agents are hydrides derived from aluminum and boron.

$LiAlH_4$ is a very reactive reducing agent and it reduces most carbonyl groups. $NaBH_4$ and $Ca(BH_4)_2$ are much milder agents than $LiAlH_4$ and can be used to selectively reduce carbonyl compounds. When I tried to reduce the ester group, $LiAlH_4$ was more efficient than $NaBH_4$. To enhance the chemical yield, I used the diisobutylaluminum hydride (DIBAL-H) which is known as a very efficient reducing agent. Yet, I found that $LiAlH_4$ was still more effective than DIBAL-H in reducing the ester group.

2. The advantages of [^{18}F]MEFWAY

First, the radiochemical yield of [^{18}F]MEFWAY is higher than that of [^{18}F]FCWAY. The radiofluorination [^{18}F]FCWAY occurs at the aromatic and secondary positions compared with the aliphatic and primary positions in [^{18}F]MEFWAY. The substrate plays the most important part in determining the reaction rate. This is because the nucleophile attacks from behind of the substrate, thus breaking the carbon-leaving group bond and forming the carbon-nucleophile bond. Therefore, to maximize the rate of the reaction, the back of the substrate must be as unhindered as possible. Overall, this means that methyl and primary substrates react the fastest, followed by secondary substrates. Therefore, the radiochemical yield of [^{18}F]MEFWAY is higher than that of [^{18}F]FCWAY.

A radioprobe and its precursor must have enough and reproducible synthetic yield to perform PET experiments. For example, although [*carbonyl*-^{11}C]Desmethyl-WAY-100635 ([^{11}C]DWAY) made up for the fast-metabolism of WAY-100635, the radiocompound has not expanded to clinical trial due to its extremely low yield[7]. [^{18}F]FCWAY had the same problem and thus this compound was used in only one research center.

The second merit of [^{18}F]MEFWAY is in its use of ^{18}F. C-11 based radioligands have limited utility due to C-11's short half-life ($t_{1/2}$ = 20 min). Thereby, PET facilities with no cyclotron have difficulty acquiring such radioligands from distant cyclotron centers[79]. To accurate quantification of hippocampal 5-HT_{1A} levels, longer scan times (>2 h) is required because the equilibrium time of the radioligand to the 5-HT_{1A} receptors is appeared at above 2 h , thus further limiting the utility of C-11 radioligands.

Finally, [^{18}F]MEFWAY PET can serve an useful tool in animal research, providing the possibility of reducing the number of smaller animals required in longitudinal studies. In special situation such as unilateral lesion study, the reproducibility of data from imaging studies may actually be better than that obtained from traditional invasive techniques because each animal serves as its own control. [^{18}F]MEFWAY PET provides a bridge from animal research to human research and the clinic.

3. Biological evaluation of [^{18}F]MEFWAY

A. *Cis*- and *trans*-isomers of [^{18}F]MEFWAY

When the substituents found on cyclohexane are located in the same direction, the diasteromer is referred to as *cis*. In contrast, when the substituents are oriented in opposing directions, the diasteromer is referred to as *trans*. These *cis* and *trans* isomers often have different physical properties. For example, the isomers of *trans*- and *cis*-[^{18}F]FCWAY showed significant differences in 5-HT$_{1A}$ binding with reported IC_{50} values of 1.7 and 21 nM, respectively. *In vivo* PET measures of [^{18}F]FCWAY, hippocampus-to-cerebellum ratios were 19.3 and 3.6 for *trans*- and *cis*-isomers, respectively[32,80]. In the case of [^{18}F]MEFWAY, it was previously identified that the *cis*-isomer has relatively low affinity to 5-HT$_{1A}$ receptors and low specific binding compared to *trans*-isomer[81,82]. This fact is why I chose the *trans*-[^{18}F]MEFWAY.

B. Inhibition of [^{18}F]MEFWAY defluorination *in vivo*

It has been reported that [^{18}F]FCWAY is defluorinated by CYP2E1 in rats and in humans, and that this phenomenon could be blocked by pretreatment with antifungal agents (i.e. miconazole) or disulfiram[39,40]. At first, I thought that if [^{18}F]MEFWAY was defluorinated *in vivo*, CYP2E1 might be a major metabolizing enzyme of [^{18}F]MEFWAY because this radioprobe was derived from [^{18}F]FCWAY. I tested antifungal agents such as miconazole as anti-defluorination drug *in vivo*[66-68]. Disulfiram and its active metabolites have numerous side effects, such as cognitive changes, headaches and non-specific gastrointestinal symptoms[83], whereas antifungal drugs bearing imidazole moiety are known inhibitors of hepatic microsomal enzymes, especially of the CYP3A group. Therefore, I tested only antifungal agents as metabolism inhibitors of MEFWAY.

It was previously reported that miconazole was a potent inhibitor of CYP2E1[68], whereas fluconazole was not. In this research, fluconazole showed a more powerful suppression ability of defluorination than miconazole *in vivo*. Therefore, these results implied that another specific CYP450 enzyme was involved with the metabolism of [^{18}F]MEFWAY besides the already known defluorination enzymes or alternatively, suggested that an unknown anti-defluorination mechanism exists in living systems. Another possible defluorination enzyme is glutathione *S*-transferase. It has been reported that this enzyme plays a crucial role in the radiodefluorination

of 3-fluoro-5-(2-(2-^{18}F-(fluoromethyl)-thiazol-4-yl)ethynyl)benzonitrile ([^{18}F]SP 203), a metabotropic glutamate receptor subtype 5 (mGluR5) antagonist radioligand[84]. Further study will be needed to be identify this defluorination enzyme and its mechanism.

Fluconazole has some advantages over other drugs in terms of pharmacological and pharmacokinetic properties. Firstly, it has high water solubility. Miconazole is a synthetic lipophilic imidazole compound, so it requires a proper vehicle system for intravenous injection, and the Food and Drug Administration does not approve of oral or intravenous administration of miconazole in the United States. Secondly, it can be used in both preclinical and clinical studies. Lastly, it suffers minimal metabolism, and has excellent bioavailability with relatively low toxicity compared with miconazole[85].

4. Application to animal disease models

A. Acute model of depression

This study demonstrated that forced swimming stimulus induces the down-regulation of the post-synaptic 5-HT_{1A} receptors. It may be hypothesized that the

strong stimuli such as forced swimming develops an enhanced inhibitory ability of the dorsal raphe serotonergic neurons leading to the a reduction of the 5-HT neurotransmission. Then, 5-HT level was decreased in the post-synaptic region[86], it may subsequently lead to a reduction of the hippocampal 5-HT_{1A} receptor densities in the plasma membrane. This finding is consistent with the previous results. *In vitro* binding assay in rats demonstrated that this stimuli causes a down-regulation of the 5-HT_{1A} receptors in the hippocampus, and a slight up-regulation of the 5-HT_{1A} receptors in the frontal cortex[76]. Investigation of the brain glucose metabolism using [^{18}F]FDG microPET in the forced swimming model showed the significant deactivation in the hippocampus[87]. These 5-HT_{1A} receptor functions were also observed in depressed patients[88,89].

The hippocampus is involved in the regulation of acute stress. Prussner el al. proposed that the hippocampus is elevated activation during non-stressful situation whereas the its activity is decreased during stressful state[90]. From this perspective, the decrease of the BP_{ND} in the hippocampus presented here seems to reflect involvement of this area in response to forced swimming stress.

B. Hemi-Parkinson's model.

Present research demonstrated that unilateral 6-OHDA lesion induces bilaterally down-regulation of the hippocampal 5-HT_{1A} receptors and this finding is

corresponds with the previous report that 6-OHDA lesion induced the bilaterally down-regulation of 5-HT_{2A} receptors in cortical area[77]. The previous reports showed that the unilateral 6-OHDA lesion induces dramatic bilateral depletion of 5-HT in the hippocampus[91-94] and that deactivated glucose metabolism in hippocampus was observed in an immobilizations stress[95]. In addition, Winter et al. proposed that lesion of dopaminergic neurons induced depressive-like behavior in rats[93] .

Depression in PD is a common complication. Approximately 40 % of patients with Parkinson's disease (PD) have suffered from depression growing evidence suggest that the serotonergic system dysfunction is involved in the pathophysiology of PD[60,96]. Decreased contents of 5-HT and its major metabolite 5-HIAA in the basal ganglia, raphe nuclei, cerebral cortex and CSF have been demonstrated in PD patients[56,97,98,99]. Functional imaging studies have reported the reduction of 5-HT_{1A} receptor densities in the raphe nuclei and the hippocampus in PD patients[61,100].

V. CONCLUSION

In the present study I established an efficient synthetic method of [^{18}F]MEFWAY and confirmed that [^{18}F]MEFWAY is a useful radioligand to measure the change in postsynaptic 5-HT_{1A} receptor density.

An efficient synthetic method for the preparation of [^{18}F]MEFWAY

(1) This method consists of an acid chloride coupling reaction to activate the carboxylic acid and proper reduction condition (i.e. $LiAlH_4$/diethyl ether) to suppress breakdown of the amide bond. The synthesis yield using this protocol was dramatically increased from 8% to 45 %.

Evaluation of the efficacy of [^{18}F]MEFWAY in small animal

(1) Control [^{18}F]MEFWAY showed severe skull uptake due to defluorination *in vivo*.

(2) Pretreatment of fluconazole (60 mg/kg) before injection of [^{18}F]MEFWAY suppressed the skull uptake by 81% compared to the control.

(3) In the pre-block and displacement experiments, specificity of [^{18}F]MEFWAY to 5-HT$_{1A}$ receptors was confirmed.

Application in the animal disease models

(1) When [^{18}F]MEFWAY is applied in known animal disease models, this radioprobe successfully detected the changes in the 5-HT$_{1A}$ receptor density.

These results showed that [^{18}F]MEFWAY is a useful PET radioligand to examine the changes in 5-HT$_{1A}$ receptor density *in vivo*.

REFERENCES

1. Kepe V, Barrio JR, Huang SC, Ercoli L, Siddarth P, Shoghi-Jadid K, et al. Serotonin 1A receptors in the living brain of Alzheimer's disease patients. Proc Natl Acad Sci U S A 2006;103:702-7.
2. Lanzenberger RR, Mitterhauser M, Spindelegger C, Wadsak W, Klein N, Mien LK, et al. Reduced serotonin-1A receptor binding in social anxiety disorder. Biol Psychiatry 2007;61:1081-9.
3. Akimova E, Lanzenberger R, Kasper S. The serotonin-1A receptor in anxiety disorders. Biol Psychiatry 2009;66:627-35.
4. Drevets WC, Thase ME, Moses-Kolko EL, Price J, Frank E, Kupfer DJ, et al. Serotonin-1A receptor imaging in recurrent depression: replication and literature review. Nucl Med Biol 2007;34:865-77.
5. Moses-Kolko EL, Wisner KL, Price JC, Berga SL, Drevets WC, Hanusa BH, et al. Serotonin 1A receptor reductions in postpartum depression: a positron emission tomography study. Fertil Steril 2008;89:685-92.
6. Yasuno F, Suhara T, Ichimiya T, Takano A, Ando T, Okubo Y. Decreased 5-HT1A receptor binding in amygdala of schizophrenia. Biol Psychiatry 2004;55:439-44.
7. Kumar JS, Mann JJ. PET tracers for 5-HT(1A) receptors and uses thereof. Drug Discov Today 2007;12:748-56.

8. Grasby PM, Bench C. Neuroimaging of mood disorders. Current Opinion in Psychiatry 1997;10:73-8.

9. Fumita M, Innis RB. In vivo molecular imaging: ligand development and research application. Neuropharmarm; 2000.

10. Rapport MM, Green AA, Page IH. Crystalline serotonin. Science 1948;108:329-30.

11. Erspamer V. Pharmacology of enteramine. I. Action of acetone extract of rabbit stomach mucosa on blood pressure and on surviving isolated organs. Neuro Soc Arch Exp Pathol Phamacol 1940;196:343-65.

12. Erspamer V, Asero B. Identification of enteramine, the specific hormone of the enterochromaffin cell system, as 5-hydroxytryptamine. Nature 1952;169:800-1.

13. Twarog BM. Serotonin: history of a discovery. Comp Biochem Physiol C 1988;91:21-4.

14. Zigmond MJ. Fundamental neuroscience. San Diego: Academic Press; 1999.

15. Agnati LF, Fuxe K, Hokfelt T, Benfenati F, Calza L, Johansson O, et al. Morphometric characterization of transmitter-identified nerve cell groups: analysis of mesencephalic 5-HT nerve cell bodies. Brain Res Bull 1982;9:45-51.

16. Hoyer D, Clarke DE, Fozard JR, Hartig PR, Martin GR, Mylecharane EJ, et al. International Union of Pharmacology classification of receptors for 5-hydroxytryptamine (Serotonin). Pharmacol Rev 1994;46:157-203.

17. Corradetti R, Pugliese AM. Electrophysiological effects of felbamate. Life Sci 1998;63:1075-88.

18. Hall H, Lundkvist C, Halldin C, Farde L, Pike VW, McCarron JA, et al. Autoradiographic localization of 5-HT1A receptors in the post-mortem human brain using [3H]WAY-100635 and [11C]way-100635. Brain Res 1997;745:96-108.

19. Sotelo C, Cholley B, El Mestikawy S, Gozlan H, Hamon M. Direct Immunohistochemical Evidence of the Existence of 5-HT1A Autoreceptors on Serotoninergic Neurons in the Midbrain Raphe Nuclei. Eur J Neurosci 1990;2:1144-54.

20. Rabiner EA, Bhagwagar Z, Gunn RN, Sargent PA, Bench CJ, Cowen PJ, et al. Pindolol augmentation of selective serotonin reuptake inhibitors: PET evidence that the dose used in clinical trials is too low. Am J Psychiatry 2001;158:2080-2.

21. Okarvi SM. Recent progress in fluorine-18 labelled peptide radiopharmaceuticals. Eur J Nucl Med 2001;28:929-38.

22. Miller PW, Long NJ, Vilar R, Gee AD. Synthesis of 11C, 18F, 15O, and 13N radiolabels for positron emission tomography. Angew Chem Int Ed Engl 2008;47:8998-9033.

23. Schubiger PA, Lehmann L, Friebe M. PET chemistry : the driving force in molecular imaging. Berlin New York: Springer; 2007.

24. Ido T, Wan CN, Castella V, Fowler JS, Wolf AP, Reivich M, et al. Labeled 2-deoxy-D-glucose analogs: 18F-labeled 2-deoxy-2-fluoro-D-glucose, 2-deoxy-2-fluoro-D-mannose and 14C-2-deoxy-2-fluoro-D-glucose". J Labeled Compounds Radiopharm J Labeled Compounds Radiopharm 1978;24:174-83.

25. Scott DJ, Stohler CS, Koeppe RA, Zubieta JK. Time-course of change in [11C]carfentanil and [11C]raclopride binding potential after a nonpharmacological challenge. Synapse 2007;61:707-14.

26. Mukherjee J, Yang ZY, Das MK, Brown T. Fluorinated benzamide neuroleptics--III. Development of (S)-N-[(1-allyl-2-pyrrolidinyl)methyl]-5-(3-[18F]fluoropropyl)-2, 3-dimethoxybenzamide as an improved dopamine D-2 receptor tracer. Nucl Med Biol 1995;22:283-96.

27. Rasey JS, Grunbaum Z, Magee S, Nelson NJ, Olive PL, Durand RE, et al. Characterization of Radiolabeled Fluoromisonidazole as a Probe for Hypoxic Cells. Radiation Research 1987;111:292-304.

28. Pike VW. PET radiotracers: crossing the blood-brain barrier and surviving metabolism. Trends Pharmacol Sci 2009;30:431-40.

29. Karramkam M, Hinnen F, Berrehouma M, Hlavacek C, Vaufrey F, Halldin C, et al. Synthesis of a [6-pyridinyl-18F]-labelled fluoro derivative of WAY-100635 as a candidate radioligand for brain 5-HT1A receptor imaging with PET. Bioorg Med Chem 2003;11:2769-82.

30. Kung HF, Stevenson DA, Zhuang ZP, Kung MP, Frederick D, Hurt SD. New 5-HT1A receptor antagonist: [3H]p-MPPF. Synapse 1996;23:344-6.

31. Lang L, Jagoda E, Ma Y, Sassaman MB, Eckelman WC. Synthesis and in vivo biodistribution of F-18 labeled 3-cis-, 3-trans-, 4-cis-, and 4-trans-fluorocyclohexane derivatives of WAY 100635. Bioorg Med Chem 2006;14:3737-48.

32. Lang L, Jagoda E, Schmall B, Sassaman M, Ma Y, Eckelman WC. Fluoro analogs of WAY-100635 with varying pharmacokinetics properties. Nucl Med Biol 2000;27:457-62.

33. Marchais-Oberwinkler S, Nowicki B, Pike VW, Halldin C, Sandell J, Chou YH, et al. N-oxide analogs of WAY-100635: new high affinity 5-HT(1A) receptor antagonists. Bioorg Med Chem 2005;13:883-93.

34. McCarron JA, Pike VW, Halldin C, Sandell J, Sovago J, Gulyas B, et al. The pyridinyl-6 position of WAY-100635 as a site for radiofluorination--

effect on 5-HT1A receptor radioligand behavior in vivo. Mol Imaging Biol 2004;6:17-26.

35. Sandell J, Halldin C, Pike VW, Chou YH, Varnas K, Hall H, et al. New halogenated [11C]WAY analogues, [11C]6FPWAY and [11C]6BPWAY--radiosynthesis and assessment as radioligands for the study of brain 5-HT1A receptors in living monkey. Nucl Med Biol 2001;28:177-85.

36. Wilson AA, DaSilva JN, Houle S. [18F]fluoroalkyl analogues of the potent 5-HT1A antagonist WAY 100635: radiosyntheses and in vivo evaluation. Nucl Med Biol 1996;23:487-90.

37. Gunn RN, Sargent PA, Bench CJ, Rabiner EA, Osman S, Pike VW, et al. Tracer kinetic modeling of the 5-HT1A receptor ligand [carbonyl-11C]WAY-100635 for PET. Neuroimage 1998;8:426-40.

38. Lang L, Jagoda E, Schmall B, Vuong BK, Adams HR, Nelson DL, et al. Development of fluorine-18-labeled 5-HT1A antagonists. J Med Chem 1999;42:1576-86.

39. Ryu YH, Liow JS, Zoghbi S, Fujita M, Collins J, Tipre D, et al. Disulfiram inhibits defluorination of (18)F-FCWAY, reduces bone radioactivity, and enhances visualization of radioligand binding to serotonin 5-HT1A receptors in human brain. J Nucl Med 2007;48:1154-61.

40. Tipre DN, Zoghbi SS, Liow JS, Green MV, Seidel J, Ichise M, et al. PET imaging of brain 5-HT1A receptors in rat in vivo with 18F-FCWAY and

improvement by successful inhibition of radioligand defluorination with miconazole. J Nucl Med 2006;47:345-53.

41. Carson RE, Lang L, Watabe H, Der MG, Adams HR, Jagoda E, et al. PET evaluation of [(18)F]FCWAY, an analog of the 5-HT(1A) receptor antagonist, WAY-100635. Nucl Med Biol 2000;27:493-7.

42. Saigal N, Pichika R, Easwaramoorthy B, Collins D, Christian BT, Shi B, et al. Synthesis and biologic evaluation of a novel serotonin 5-HT1A receptor radioligand, 18F-labeled mefway, in rodents and imaging by PET in a nonhuman primate. J Nucl Med 2006;47:1697-706.

43. Paterson LM, Kornum BR, Nutt DJ, Pike VW, Knudsen GM. 5-HT radioligands for human brain imaging with PET and SPECT. Med Res Rev 2011.

44. Nestler EJ, Barrot M, DiLeone RJ, Eisch AJ, Gold SJ, Monteggia LM. Neurobiology of depression. Neuron 2002;34:13-25.

45. Huang EJ, Reichardt LF. Neurotrophins: roles in neuronal development and function. Annu Rev Neurosci 2001;24:677-736.

46. Monteleone P, Serritella C, Martiadis V, Maj M. Decreased levels of serum brain-derived neurotrophic factor in both depressed and euthymic patients with unipolar depression and in euthymic patients with bipolar I and II disorders. Bipolar Disord 2008;10:95-100.

47. Sen S, Duman R, Sanacora G. Serum brain-derived neurotrophic factor, depression, and antidepressant medications: meta-analyses and implications. Biol Psychiatry 2008;64:527-32.

48. Smith MA, Makino S, Kvetnansky R, Post RM. Stress and glucocorticoids affect the expression of brain-derived neurotrophic factor and neurotrophin-3 mRNAs in the hippocampus. J Neurosci 1995;15:1768-77.

49. Lonze BE, Ginty DD. Function and regulation of CREB family transcription factors in the nervous system. Neuron 2002;35:605-23.

50. Ren X, Dwivedi Y, Mondal AC, Pandey GN. Cyclic-AMP response element binding protein (CREB) in the neutrophils of depressed patients. Psychiatry Res 2011;185:108-12.

51. Meyer JH, Ginovart N, Boovariwala A, Sagrati S, Hussey D, Garcia A, et al. Elevated monoamine oxidase a levels in the brain: an explanation for the monoamine imbalance of major depression. Arch Gen Psychiatry 2006;63:1209-16.

52. van Praag HM. Depression. Lancet 1982;2:1259-64.

53. van Praag HM, de Haan S. Central serotonin metabolism and frequency of depression. Psychiatry Res 1979;1:219-24.

54. Lopez JF, Chalmers DT, Little KY, Watson SJ. A.E. Bennett Research Award. Regulation of serotonin1A, glucocorticoid, and mineralocorticoid

receptor in rat and human hippocampus: implications for the neurobiology of depression. Biol Psychiatry 1998;43:547-73.

55. Bowen DM, Najlerahim A, Procter AW, Francis PT, Murphy E. Circumscribed changes of the cerebral cortex in neuropsychiatric disorders of later life. Proc Natl Acad Sci U S A 1989;86:9504-8.

56. Scatton B, Javoy-Agid F, Rouquier L, Dubois B, Agid Y. Reduction of cortical dopamine, noradrenaline, serotonin and their metabolites in Parkinson's disease. Brain Res 1983;275:321-8.

57. Shannak K, Rajput A, Rozdilsky B, Kish S, Gilbert J, Hornykiewicz O. Noradrenaline, dopamine and serotonin levels and metabolism in the human hypothalamus: observations in Parkinson's disease and normal subjects. Brain Res 1994;639:33-41.

58. Kish SJ, Tong J, Hornykiewicz O, Rajput A, Chang LJ, Guttman M, et al. Preferential loss of serotonin markers in caudate versus putamen in Parkinson's disease. Brain 2008;131:120-31.

59. Guttman M, Boileau I, Warsh J, Saint-Cyr JA, Ginovart N, McCluskey T, et al. Brain serotonin transporter binding in non-depressed patients with Parkinson's disease. Eur J Neurol 2007;14:523-8.

60. Albin RL, Koeppe RA, Bohnen NI, Wernette K, Kilbourn MA, Frey KA. Spared caudal brainstem SERT binding in early Parkinson's disease. J Cereb Blood Flow Metab 2008;28:441-4.

61. Doder M, Rabiner EA, Turjanski N, Lees AJ, Brooks DJ. Tremor in Parkinson's disease and serotonergic dysfunction: an 11C-WAY 100635 PET study. Neurology 2003;60:601-5.

62. Ungerstedt U. Postsynaptic supersensitivity after 6-hydroxy-dopamine induced degeneration of the nigro-striatal dopamine system. Acta Physiol Scand Suppl 1971;367:69-93.

63. Glinka Y, Gassen M, Youdim MB. Mechanism of 6-hydroxydopamine neurotoxicity. J Neural Transm Suppl 1997;50:55-66.

64. Gonzalez FJ. Molecular genetics of the P-450 superfamily. Pharmacol Ther 1990;45:1-38.

65. Jefcoate CR. Measurement of substrate and inhibitor binding to microsomal cytochrome P-450 by optical-difference spectroscopy. Methods Enzymol 1978;52:258-79.

66. Blum RA, Wilton JH, Hilligoss DM, Gardner MJ, Henry EB, Harrison NJ, et al. Effect of fluconazole on the disposition of phenytoin. Clin Pharmacol Ther 1991;49:420-5.

67. Maurice M, Pichard L, Daujat M, Fabre I, Joyeux H, Domergue J, et al. Effects of imidazole derivatives on cytochromes P450 from human hepatocytes in primary culture. FASEB J 1992;6:752-8.

68. Tassaneeyakul W, Birkett DJ, Miners JO. Inhibition of human hepatic cytochrome P4502E1 by azole antifungals, CNS-active drugs and non-steroidal anti-inflammatory agents. Xenobiotica 1998;28:293-301.

69. George P, Watson C. The Rat Brain in Stereotaxic Coordinates. 6th ed. 6 ed. San Diego,CA: Academic Press; 2007.

70. Pazos A, Palacios JM. Quantitative autoradiographic mapping of serotonin receptors in the rat brain. I. Serotonin-1 receptors. Brain Res 1985;346:205-30.

71. el Mestikawy S, Riad M, Laporte AM, Verge D, Daval G, Gozlan H, et al. Production of specific anti-rat 5-HT1A receptor antibodies in rabbits injected with a synthetic peptide. Neurosci Lett 1990;118:189-92.

72. Blum D, Torch S, Lambeng N, Nissou M, Benabid AL, Sadoul R, et al. Molecular pathways involved in the neurotoxicity of 6-OHDA, dopamine and MPTP: contribution to the apoptotic theory in Parkinson's disease. Prog Neurobiol 2001;65:135-72.

73. Glinka Y, Tipton KF, Youdim MB. Nature of inhibition of mitochondrial respiratory complex I by 6-Hydroxydopamine. J Neurochem 1996;66:2004-10.

74. Schwarting RK, Huston JP. The unilateral 6-hydroxydopamine lesion model in behavioral brain research. Analysis of functional deficits, recovery and treatments. Prog Neurobiol 1996;50:275-331.

75. Pike VW, McCarron JA, Hume SP, Ashworth S, Opacka-Jufry J, Osman S, et al. Preclinical development of a radioligand for studies of central 5-HT_{1A} receptors in vivo [^{11}C]WAY 100635. Med Chem Res 1995;5:208-77.

76. Bellido I, Gomez-Luque A, Garcia-Carrera P, Rius F, de la Cuesta FS. Female rats show an increased sensibility to the forced swim test depressive-like stimulus in the hippocampus and frontal cortex 5-HT1A receptors. Neurosci Lett 2003;350:145-8.

77. Li Y, Huang XF, Deng C, Meyer B, Wu A, Yu Y, et al. Alterations in 5-HT2A receptor binding in various brain regions among 6-hydroxydopamine-induced Parkinsonian rats. Synapse 2010;64:224-30.

78. Christian AGN, Montalbetti, Falque V. Amide bond formation and peptide coupling. Tetrahedron 2005;61:10827-52.

79. Brust P, Hinz R, Kuwabara H, Hesse S, Zessin J, Pawelke B, et al. In vivo measurement of the serotonin transporter with (S)-([18F]fluoromethyl)-(+)-McN5652. Neuropsychopharmacology 2003;28:2010-9.

80. Lang L, Jagoda E, Schmall B, Sassaman M, Magata Y, Eckelman WC. Comparison of ^{18}F labeled *cis* and *trans* 4-fluorocyclohexane derivatives of WAY-100635 J Nucl Med 1999;40:37P-8P.

81. Saigal N, Pichika R, Easwaramoorthy B, Mukherjee J. Serotonin competition with the new 5-HT_{1A} receptor PET radiotracer: [^{18}F]mefway. J Nucl Med 2006;47:281P.

82. Wooten D, Hillmer A, Murali D, Barnhart T, Schneider ML, Mukherjee J, et al. An in vivo comparison of cis- and trans-[18F]mefway in the nonhuman primate. Nucl Med Biol 2011;38:925-32.

83. Mutschler J, Dirican G, Gutzeit A, Grosshans M. Safety and efficacy of long-term disulfiram aftercare. Clin Neuropharmacol 2011;34:195-8.

84. Shetty HU, Zoghbi SS, Simeon FG, Liow JS, Brown AK, Kannan P, et al. Radiodefluorination of 3-fluoro-5-(2-(2-[18F](fluoromethyl)-thiazol-4-yl)ethynyl)benzonitrile ([18F]SP203), a radioligand for imaging brain metabotropic glutamate subtype-5 receptors with positron emission tomography, occurs by glutathionylation in rat brain. J Pharmacol Exp Ther 2008;327:727-35.

85. Brammer KW, Farrow PR, Faulkner JK. Pharmacokinetics and tissue penetration of fluconazole in humans. Rev Infect Dis 1990;12 Suppl 3:S318-26.

86. Kirby LG, Allen AR, Lucki I. Regional differences in the effects of forced swimming on extracellular levels of 5-hydroxytryptamine and 5-hydroxyindoleacetic acid. Brain Res 1995;682:189-96.

87. Jang DP, Lee SH, Lee SY, Park CW, Cho ZH, Kim YB. Neural responses of rats in the forced swimming test: [F-18]FDG micro PET study. Behav Brain Res 2009;203:43-7.

88. Stockmeier CA, Dilley GE, Shapiro LA, Overholser JC, Thompson PA, Meltzer HY. Serotonin receptors in suicide victims with major depression. Neuropsychopharmacology 1997;16:162-73.

89. Arango V, Underwood MD, Gubbi AV, Mann JJ. Localized alterations in pre- and postsynaptic serotonin binding sites in the ventrolateral prefrontal cortex of suicide victims. Brain Res 1995;688:121-33.

90. Pruessner JC, Dedovic K, Khalili-Mahani N, Engert V, Pruessner M, Buss C, et al. Deactivation of the limbic system during acute psychosocial stress: evidence from positron emission tomography and functional magnetic resonance imaging studies. Biol Psychiatry 2008;63:234-40.

91. Pierucci M, Di Matteo V, Benigno A, Crescimanno G, Esposito E, Di Giovanni G. The unilateral nigral lesion induces dramatic bilateral modification on rat brain monoamine neurochemistry. Ann N Y Acad Sci 2009;1155:316-23.

92. Tadaiesky MT, Dombrowski PA, Figueiredo CP, Cargnin-Ferreira E, Da Cunha C, Takahashi RN. Emotional, cognitive and neurochemical alterations in a premotor stage model of Parkinson's disease. Neuroscience 2008;156:830-40.

93. Winter C, von Rumohr A, Mundt A, Petrus D, Klein J, Lee T, et al. Lesions of dopaminergic neurons in the substantia nigra pars compacta and in the

ventral tegmental area enhance depressive-like behavior in rats. Behav Brain Res 2007;184:133-41.

94. Branchi I, D'Andrea I, Armida M, Cassano T, Pezzola A, Potenza RL, et al. Nonmotor symptoms in Parkinson's disease: investigating early-phase onset of behavioral dysfunction in the 6-hydroxydopamine-lesioned rat model. J Neurosci Res 2008;86:2050-61.

95. Sung KK, Jang DP, Lee S, Kim M, Lee SY, Kim YB, et al. Neural responses in rat brain during acute immobilization stress: a [F-18]FDG micro PET imaging study. Neuroimage 2009;44:1074-80.

96. Aarsland D, Marsh L, Schrag A. Neuropsychiatric symptoms in Parkinson's disease. Mov Disord 2009;24:2175-86.

97. Paulus W, Jellinger K. The neuropathologic basis of different clinical subgroups of Parkinson's disease. J Neuropathol Exp Neurol 1991;50:743-55.

98. Mayeux R, Stern Y, Cote L, Williams JB. Altered serotonin metabolism in depressed patients with parkinson's disease. Neurology 1984;34:642-6.

99. Tohgi H, Abe T, Takahashi S, Takahashi J, Hamato H. Concentrations of serotonin and its related substances in the cerebrospinal fluid of parkinsonian patients and their relations to the severity of symptoms. Neurosci Lett 1993;150:71-4.

100. Ballanger B, Poisson A, Broussolle E, Thobois S. Functional imaging of non-motor signs in Parkinson's disease. J Neurol Sci 2012;315:9-14.

ABSTRACT (IN KOREAN)

설치류 뇌의 세로토닌 1A 수용체를 영상화하기 위해 개발된 새로운 방사성리간드인 [^{18}F]MEFWAY 의 효율적 합성과, PET 영상 및 질환모델 적용

<지도교수 김철훈>

연세대학교 대학원 의과학과

최재용

중추신경계 세로토닌 1A ($5\text{-}HT_{1A}$) 수용체 밀도의 변화는 우울증, 불안증, 정신분열증과 같은 다양한 신경정신질환과 관련이 있다. 그래서 뇌 $5\text{-}HT_{1A}$ 수용체에 대한 생체 내 영상은 신경과학에서 중요한 연구 주제가 되어 왔다 .

4-([^{18}F]fluoranylmethyl)-*N*-[2-[4-(2-methoxyphenyl)piperazin-1-yl]ethyl]-*N*-pyridin-2-ylcyclohexane-1-carboxamide ([^{18}F]MEFWAY) 는 세로토닌 1A 수용체를 영상화하기 위해 최근 개발된 방사성 리간드이다. 그러나 MEFWAY 전구체의 낮은 합성 수율로 인해 현재까지 체내에서의 생화학적, 약리학적 특성에 대한 평가는 보고되지 않았다. 본 연구에서는 생체내 연구의 적용가능성에 대한 관점에서 [^{18}F]MEFWAY 의 유용성을 평가하였다.

MEFWAY 전구체를 효율적으로 합성하기 위해 카르복실산을 활성화시키는 방법과 아미드 결합의 해리를 억제하기 위한 환원법을 도입하였다. 이 새로운 방법을 통하여 합성수율을 기존 8%에서 45% 로 크게 향상 시켰다. 이렇게 만들어진 전구체에 F-18 을 도입한 다음, 랫트 뇌에서 [^{18}F]MEFWAY 의 유효성 및 대사 안정성을 평가하였다.

[^{18}F]MEFWAY 는 탈불소화로 인해 방사능의 두개골 섭취를 나타내었다. 이러한 방사능의 두개골 섭취를 줄이기 위하여 마이코나졸과 플루코나졸을 전처리 한 결과 두개골 섭취가 각각 68%와 80% 억제되었다. 그리고, 5-HT1A 수용체의 길항제를 이용한 pre-block, displacement 를 통하여 [^{18}F]MEFWAY 가 5-HT_{1A} 수용체에 선택적인 방사성리간드임을 확인하였다.

또한 개발한 [^{18}F]MEFWAY 을 동물 질환 모델에 적용하여 보았다. 여기서 편측 6-OHDA 병소는 파킨슨 병에 대한 모델로 사용하였고, 강제 수영은 우울증을 유도하기 위해 사용하였다. 편측 6-OHDA 병소 (unilateral 6-OHDA lesion) 랫트에서 해마에 대한 결합능이 정상군 대비 양측에서 현저하게 감소하였다. 그리고 우울증 모델에서 역시 결합능의 유의할 만한 감소가 관찰되었다.

따라서 본 연구에서는 [^{18}F]MEFWAY 전구체의 우수한 합성수율을 보장하는 합성법을 개발하였고, 뇌 5-HT_{1A} 수용체에 대한 유효성을 확인하였다. 또한 동물을 이용한 질환 모델에 성공적인 적용을 입증하였다. 따라서 [^{18}F]MEFWAY 는 생체내에서 5-HT_{1A} 수용체 밀도의 변화를 평가하는 데 유용한 방사성리간드임을 시사한다.

핵심되는 말: 5-HT_{1A} 수용체, PET, 방사성리간드, 우울증, 파킨슨 병